N71-17341

NASA CR116404

APPLICATION OF RADIOACTIVE TRACER TECHNIQUES TO FLOW DECAY PROBLEMS

Interim Final Report D180-12741-1 December, 1970

Prepared for

THE JET PROPULSION LABORATORY
PASADENA, CALIFORNIA

under

NATIONAL AERONAUTICS AND SPACE
ADMINISTRATION CONTRACT NAS7-779

THE BOEING COMPANY
SEATTLE, WASHINGTON

CASE FILE
COPY

APPLICATION OF RADIOACTIVE TRACER TECHNIQUES TO FLOW DECAY PROBLEMS

INTERIM FINAL REPORT D180-12741-1 DECEMBER, 1970

Prepared for

THE JET PROPULSION LABORATORY
PASADENA, CALIFORNIA 91103
UNDER NATIONAL AERONAUTICS AND SPACE
ADMINISTRATION CONTRACT NAS7-779

THE BOEING COMPANY
SEATTLE, WASHINGTON 98124

J. R. O'Brien, Project Manager
K. E. Pullen, Principal Investigator
T. L. Smith, Research Specialist

FOREWORD

The work in this program was performed at The Boeing Company, Seattle, Washington, under NASA Contract NAS7-779 during the period March 26 - October 26, 1970. The NASA Headquarters project manager was Mr. Frank Compitello. The program was administered under the direction of the technical manager, Mr. Louis R. Toth of the Jet Propulsion Laboratory, Pasadena, California.

The project was managed at The Boeing Company by Mr. James R. O'Brien of the Flight Technology Department (Propulsion Group) of the Research Division of the Aerospace Group. The technical effort was the responsibility of Dr. Kent E. Pullen and Mr. T. Lynn Smith.

TABLE OF CONTENTS

LIST OF FIGURES

LIST OF TABLES

1.0 SUMMARY

In this program various applications of radioactive tracer techniques to flow decay problems were explored. The main object of the program was to develop a sensitive tool which could be used to detect the time, place, and degree of deposition of metal contaminants within various components of a propellant feed system. Such a tool was successfully developed and readily applied to flow studies involving nitrogen tetroxide and hydrazine.

As an analytical tool, thermal neutron activation followed by gamma counting was shown to be a sensitive method for the quantitative analysis of a variety of metals in liquid propellants. For purposes of demonstration, the experimental investigation was limited to the metals iron, zinc, and chromium and the propellants hydrazine and nitrogen tetroxide. Both "wet" and "dry" analytical methods were employed. In the wet method the propellant and its contents were activated; in the dry method the residue left after the propellant had been evaporated was activated. The dry method was found to be more widely applicable to propellants and was simpler to employ. Limits of detection of 0.1, 0.01, and 0.001 parts per million (ppm) were found for iron, zinc, and chromium respectively. These limits apply to a small amount of propellant (10 grams), a relatively short counting time (1 hour), and moderate activation conditions (10 hours in a flux of 8×10^{12} neutrons per cm^2 per sec.).

As a diagnostic tool, the gamma emissions from radioactive tracers of iron-59, zinc-65, and chromium-51 provided a very sensitive means of monitoring the movement of metal contaminants in a stainless steel flow test assembly. Flow tests were conducted with nitrogen tetroxide and hydrazine in which each propellant was flowed through both a filter (10 micron absolute, stainless steel wire mesh type) and a capillary (0.008 inch I.D., 10 inches long, 304 stainless steel). In most runs radioactive tracers were added directly to the propellant, while in some runs radioactive contamination was introduced through interaction of the propellant with radioactive metal surfaces.

Flow decay was readily observed when MSC-PPD-2A N_2O_4 was passed through the filters. In all such runs measurable radioactivity (about 1 to 10% of the total added) deposited on the filters, often prior to the time at which a decrease in flow rate could be measured. At no time did flow decay occur without the prior or concurrent build-up of radioactivity on the filter. A few runs were made with distilled MSC-PPD-2A N_2O_4 to which had been added varying amounts of ferric nitrate. The degree of flow decay was approximately proportional to the quantity of ferric nitrate added, and with no ferric nitrate added (other than 0.001 ppm of the radioactive tracer) no flow decay was observed. Distillation thus seems to offer promise as a means of eliminating flow decay.

No flow decay was observed in any runs involving the passage of N_2O_4 through capillaries and the passage of N_2H_4 through either filters or capillaries. In none of these runs was any appreciable radioactive contamination deposited, a result which is consistent with the absence of flow decay. In some runs involving capillaries, partial blockage of the capillaries occurred, but subsequent investigation indicated that the blockage resulted from the presence of extraneous particulate matter in the propellant rather than a flow decay mechanism such as gelation or metal complex formation within the capillary.

2.0 INTRODUCTION

Generally speaking, flow decay can be defined as the decrease in flow rate of a propellant as a function of time when that propellant flows through a constriction (such as a filter, valve, or orifice). More specifically, this definition has been applied to decreases in flow rate of N_2O_4 caused by the formation and/or deposition of metal compounds (in particular, iron nitrate complexes) within those constrictions.[1,2] These iron nitrate complexes are heavily solvated with solvent (N_2O_4) molecules, even to the point of forming gels. This explains in part why such small concentrations of iron in N_2O_4 (about 1 ppm) can so easily cause clogging problems.

These very small metal concentrations necessitated the use of highly sensitive detection techniques in early flow decay studies. Consequently, shortly after initial exploratory research was undertaken,[1,2] a search was made at The Boeing Company for possible detection techniques. Subsequent work was successful in demonstrating that radioactive tracing had considerable value as a highly sensitive detection technique.[3] In the Boeing study radioactive strips of iron foil were immersed in stirred samples of distilled N_2O_4 to which had been added known amounts of various impurities (H_2O, NO, NOCl). By counting the radioactivity that was transferred to the solution as a function of time, accurate rates of dissolution were measured. The method was rapid, continuous, nondestructive, and highly sensitive. Iron concentrations were successfully measured to the nearest 0.01 ppm.

Because of the promising advantages exhibited by radioactive tracers, this program was undertaken with the object of developing a sensitive, accurate tool that could be applied rapidly and nondestructively to a feed system in an effort to answer such questions as (1) whether a build-up of metal-containing deposits is occurring during propellant flow; (2) where the build-up is occurring; (3) how fast the build-up is occurring; and (4) which metals are depositing and in what proportions. This development program was to be accomplished in two tasks. Task 1, which involved the quantitative analysis of metals in propellants, developed procedures for utilizing neutron activation as an analytical technique. For purposes of demonstration, the study was limited to the metals iron, zinc, and chromium. In performing Task 1, the groundwork was laid for establishing the gamma counting methods required for Task 2. Task 2, which involved flow tests with the propellants N_2O_4 and N_2H_4, developed procedures for tracing the movement of metal compounds through constrictions such as filters and capillaries.

3.0 THEORY

Radioactive atoms contain nuclei which possess an excess of energy. These nuclei decay at a characteristic rate to a stable state by the emission of various particles or electromagnetic radiation such as alpha particles, electrons, and gamma rays. The emissions are specific to the decaying nucleus and can be used as a positive means of identifying an element. These radioactive nuclei can be prepared through a variety of nuclear reactions, a common one being the capture of a low energy (thermal) neutron by a nonradioactive nucleus. Although only a small fraction of the total number of atoms of a sample can usually be made radioactive (often less than one atom in a billion, but a known and reproducible fraction), sufficient numbers of radioactive nuclei may remain to produce a large (and countable) rate of decay, thus forming the basis for a highly sensitive analytical technique.

In deciding whether thermal neutron activation can be applied usefully to metal analyses, two important questions need to be answered: (1) can the metal be made sufficiently radioactive that a suitably large nuclear disintegration rate is attained? (2) can the resulting disintegrations be counted? These two questions are best treated separately in order to consider the various peculiarities of specific metals.

The first question is answered by considering elementary theory. The disintegration rate, dN/dt, is directly proportional to the number of radioactive atoms, N,

$$- dN/dt = \lambda N \qquad (1)$$

where λ, the proportionality constant, is known as the disintegration constant. The disintegration constant is independent of all known physical variables (e.g., temperature, magnetic fields, pressure) and is defined by the equation

$$\lambda = \ln 2/t_{1/2} \qquad (2)$$

where $t_{1/2}$ is the half life of the isotope in question.

The rate of formation of radioactive atoms, dN/dt, in a nuclear reaction is given by the equation

$$\frac{dN}{dt} = N_o \phi \sigma \tag{3}$$

where N_o is the number of atoms available to undergo activation to the radioisotope in question, ϕ is the neutron flux in neutrons per square centimeter per second, and σ is the cross section in square centimeters. (The cross section is a measure of the probability of a neutron being captured to yield the desired radioisotope and is usually given in barns, where one barn equals 10^{-24} cm^2.)

The net number of radioactive atoms formed, dN, in time dt is the number activated in the reactor less the number that decay during the activation period.

Thus, from (1) and (3)

$$dN = N_o \phi \sigma \, dt - \lambda \, Ndt$$

$$dN = (N_o \phi \sigma - \lambda N) \, dt \tag{4}$$

upon integrating (4),

$$N = \frac{1}{\lambda} N_o \phi \sigma (1 - e^{-\lambda t}) \tag{5}$$

Equation (5) gives the number of radioactive atoms present after time t in the reactor. When t is large (that is, saturation activity is reached), the rate of formation equals the rate of decay and (5) reduces to

$$N = \frac{1}{\lambda} N_o \phi \sigma \tag{6}$$

When t is small, (5) reduces to

$$N = N_o \Phi \sigma t \tag{7}$$

using the approximation $e^{-\lambda t} \approx 1 - \lambda t$. Equation (7) is valid over a wide range of conditions. For example, iron, chromium, and zinc have half lives of the order of a month or more, and the amount of decay that occurs during, say, a 10 hour activation period is practically negligible.

Substituting (7) into (1) gives the activity of the radioisotope at the end of the activation period.

$$-\frac{dN}{dt} = \lambda N_o \phi \sigma\ t \qquad (8)$$

One can then use (8) to answer the first question asked at the beginning of this section: can the metal be made sufficiently radioactive that a suitably large nuclear disintegration rate is attained? A "suitably large" disintegration rate is defined as one that produces a counting rate in detection equipment that is roughly comparable to that of natural background. If the count rate becomes less than about one tenth that of background, then counting times must be inconveniently long in order to achieve statistically significant results.

A detailed look at probability and statistics is beyond the scope of this discussion, but a quick check of some elementary conclusions can explain the relationship between the sample count rate and the background count rate. Nuclear decay is a statistical process, and the probable error in counts recorded depends both on the total number of counts and the desired confidence level. One might ask for example how many counts must be registered to establish a 5% statistical sampling error at a 90% confidence level. This means that at that number of counts there is a 90% chance that the measured number of counts is the correct value within ± 5% of the measured number. Another way of viewing the measurement is that if many such measurements are made, 90% of them would be contained within the ± 5% error limits, and 10% would be outside the error limits. It can be shown that the error limits are estimated by the equation

$$\text{Error limits} = \pm\ n\sqrt{C} \qquad (9)$$

where C is the total number of counts and n is the number of standard deviations that corresponds to the desired confidence level. At a confidence level of 90%, the value of n is 1.645. Thus the percent error in a measured number of counts, C, at a 90% confidence level is given by

$$\text{Percent error} = \frac{1.645\ \sqrt{C}}{C}(100) \qquad (10)$$

Plots of percent error against counts are given in Figure 1 for various confidence levels. Note that at a 90% confidence level that the error is only 1.7% for a relatively small 10,000 counts. Even at 1000 counts, the error is only 5.2%.

A problem occurs when background counts must also be considered. Natural background results from sources such as cosmic rays and can be reduced by increasing the amount of shielding that is employed. For the detector-counter unit used in this study, the background count rate was of the order of 2 counts per second or 120 counts per minute (cpm) in the energy range 1.0 to 1.4 Mev.

Consider now a hypothetical radioactive sample that is counted at the slow rate of 1/100 background (1.2 cpm). For how long would one have to count to achieve a 10% statistical sampling error at a 90% confidence level? If there were no background, one would require 270 counts (from Equation 10 or Figure 1), or about 225 minutes at a count rate of 1.2 cpm. However, in the presence of a 120 cpm background, the contribution to the counts due to the background for a 225 minute count would be 120 x 225 = 27,000. Since the uncertainty in the 27,000 count background (± 270 counts from Equation (9)), is equal to the counts from the radioactive sample, a counting time of 225 minutes is completely inadequate if one desires to count the radioactive sample with a probable 10% error. One would have to count at least 100 times as long, or 22,500 minutes, to achieve about a 10% error. At this very long counting time the probable error in the background (± 2700 out of 2,700,000 counts) would be 10% of the counts of the radioactive sample (1.2 x 22,500 = 27,000). However, 22,500 minutes (a little less than 16 days) is an inconveniently lengthy time to have to count a sample.

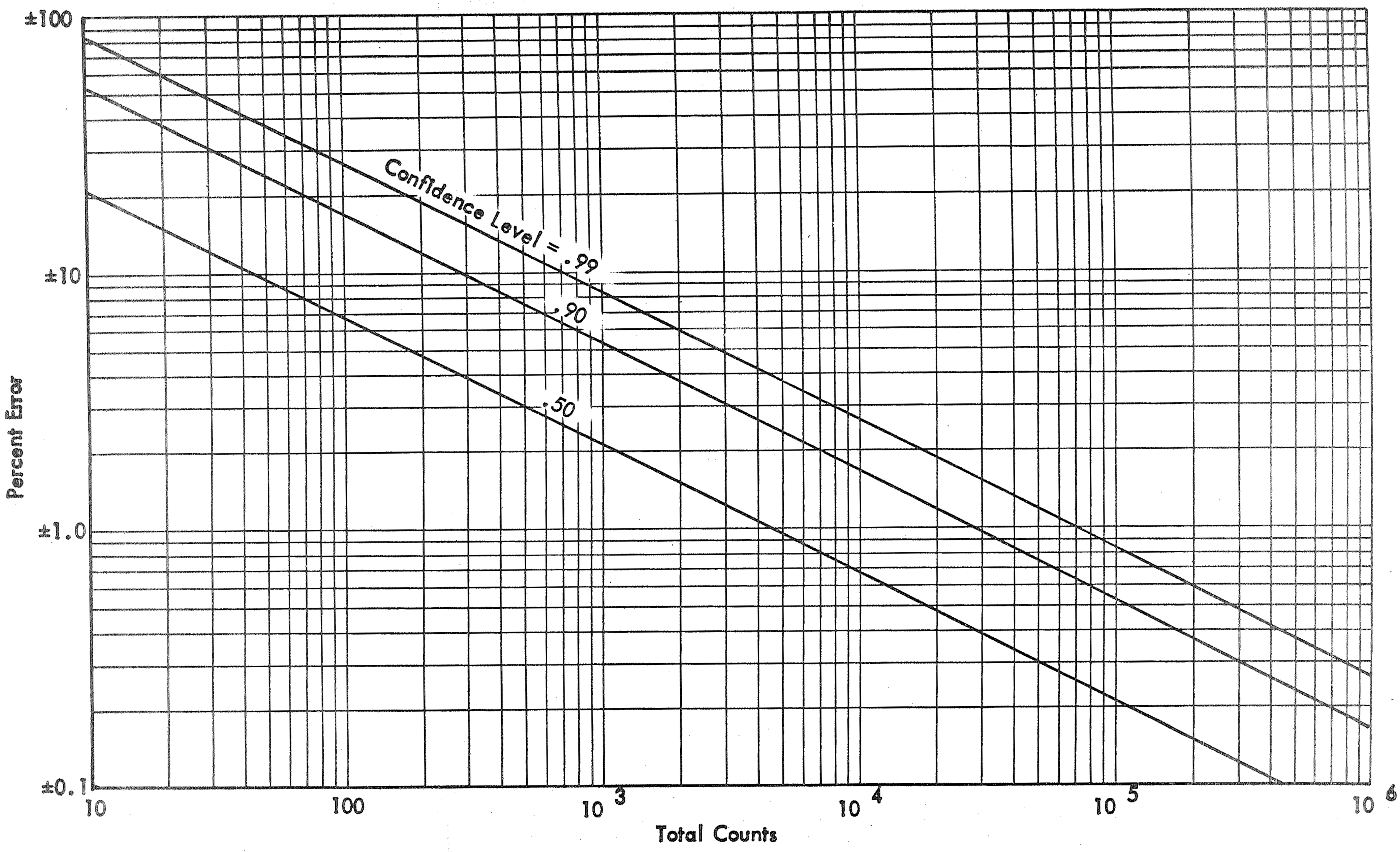

Figure 1: STATISTICAL COUNTING ERRORS

The second question asked at the beginning of this section (can the resulting disintegrations be counted?) will now be related to the first question (can a suitably large disintegration rate be attained?). A great deal depends on what type of emission is being counted. This study was restricted to the counting of gammas. Gamma rays are very penetrating and are easily counted. By contrast charged particles such as betas interact readily with matter and may possess low penetrability. Consequently, betas can be counted with greater effort and at a sacrifice in sensitivity. Fortunately, practically all common metals have at least one gamma-emitting isotope that can be prepared, if not by thermal neutron activation, then by some other means.

It must be understood that one disintegration does not correspond to one count. For some isotopes only a fraction of the disintegrations yield gammas. Consider chromium-51, iron-59, and zinc-65, the only gamma emitters formed by the thermal neutron activation of any naturally occurring isotopes of these metals.

$$_{24}Cr^{50} \text{ (4.4\% abundance)} + {}_{o}n^{1} \xrightarrow{\sigma = 16 \text{ barns}} {}_{24}Cr^{51}$$

$$_{26}Fe^{58} \text{ (0.33\% abundance)} + {}_{o}n^{1} \xrightarrow{\sigma = 1 \text{ barn}} {}_{26}Fe^{59}$$

$$_{30}Zn^{64} \text{ (48.9\% abundance)} + {}_{o}n^{1} \xrightarrow{\sigma = 0.5 \text{ barn}} {}_{30}Zn^{65}$$

The radioisotopes thus formed subsequently decay largely by the following schemes:

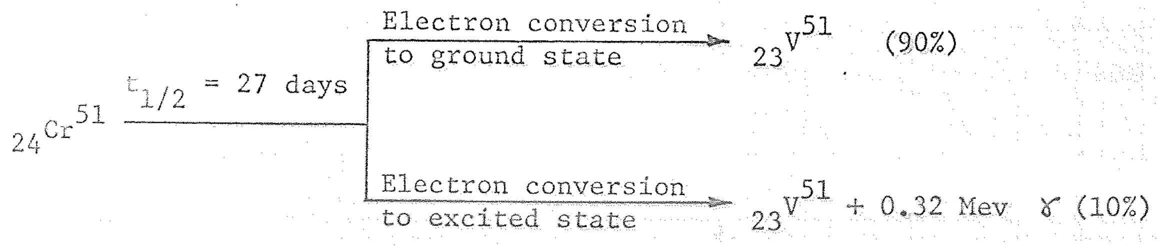

$${}_{26}\text{Fe}^{59} \xrightarrow[\beta^- \text{ emission}]{t_{1/2} = 45 \text{ days}} {}_{27}\text{Co}^{59} + \begin{cases} 1.10 \text{ Mev } \gamma & (57\%) \\ 1.29 \text{ Mev } \gamma & (43\%) \end{cases}$$

$${}_{30}\text{Zn}^{65} \xrightarrow{t_{1/2} = 245 \text{ days}} \begin{cases} \xrightarrow{\beta^+ \text{ emission}} {}_{29}\text{Cu}^{65} & (1.5\%) \\ \xrightarrow[\text{to ground state}]{\text{Electron conversion}} {}_{29}\text{Cu}^{65} & (53\%) \\ \xrightarrow[\text{to excited state}]{\text{Electron conversion}} {}_{29}\text{Cu}^{65} + 1.12 \text{ Mev } \gamma & (45.5\%) \end{cases}$$

These decay processes involve charged particle interactions followed by gamma emission. Chromium-51 decays by electron conversion, giving one 0.32 Mev gamma for every ten disintegrations. Iron-59, however, decays by beta emission giving two gammas of about 1 Mev energy in varying proportions. In one type of disintegration (57% of the time) a 1.10 Mev gamma is emitted, while in the remaining 43% of the disintegrations, a 1.29 Mev gamma is emitted. Thus, if one counts the 1.29 Mev gamma emissions, one will be able to record no more than 43 counts out of every 100 disintegrations. Zinc-65 decays in a fairly complicated manner, proceeding by positron emission (1.5%), electron conversion to the ground state (53%), and electron conversion to an excited state (45.5%) with accompanying 1.12 Mev gamma emission.

It must also be understood that a detector-counter unit is not 100% efficient. This is because of imperfections in the equipment, geometrical considerations that limit the number of gammas that can be captured by the detector, and the penetrability of gammas which permits some gammas to pass unhindered through the detector.

A beam of gammas of intensity I_o is attenuated in accordance with the equation

$$I = I_o e^{-\mu x} \qquad (11)$$

where I is the intensity after passing a distance x through the material. The linear absorption coefficient, μ, is a function of the material and the energy of gammas. For example, for 1 Mev gammas passing through metallic aluminum, μ is 0.43 inch^{-1}. This means that the beam intensity is attenuated by a factor of 2 for each 1.6 inches of aluminum through which the beam passes. In general penetrability decreases with decreasing gamma energy, so that the detector efficiency for, say, Cr^{51} gammas (0.32 Mev) is higher than for Zn^{65} gammas (1.12 Mev).

The above limitations on detector efficiency operate together to make the 3 inch x 3 inch cylindrical NaI well detector used in this study only about 15% efficient for 1 Mev gammas.

The questions asked at the beginning of this section will now be answered for the metals chromium, iron, and zinc. For purposes of illustration, the detection limit for the activation analysis of zinc will be calculated in detail. Calculations for iron, chromium, and other metals are similar.

Assume a flux of 8×10^{12} neutrons/cm^2/sec (the flux encountered in the Washington State University reactor during this program), an activation time of 36,000 seconds (10 hours is about the maximum time the reactor can be continuously run during one working day), and that a sample count rate of one tenth background (0.2 count per second) is the minimum count rate that will permit counting times of reasonable length (no more than a few hours). Since the detector efficiency is about 15% for 1 Mev gammas and since only 46% of the disintegrations yield the countable 1.12 Mev gamma, a disintegration rate slightly greater than the background count rate is required ($-dN/dt = (0.2)/(0.15)(0.46) = 2.9$ dis./sec.).

If one then substitutes the above numbers along with the proper Zn^{64} cross section ($\sigma = 0.5 \times 10^{-24}$ cm^2) and Zn^{65} disintegration constant ($\lambda = 3.275 \times 10^{-8}$ sec^{-1}) into equation (8), a value of $N_o = 6.15 \times 10^{14}$ Zn^{65} atoms is obtained. The detection limit in grams is then given by

$$\text{limit in grams} = \frac{(N_o)}{(f)}\frac{(W)}{(A)} = \frac{(6.15 \times 10^{14})}{(.489)}\frac{(65.38)}{(6.02 \times 10^{23}}$$

$$= 1.36 \times 10^{-7} \text{ g}$$

where W is the atomic weight of zinc, f is the fractional natural abundance of zinc-64, and A is Avogadro's number. Since the NaI detector well used in this study had a usable volume of about 15cc (corresponding to about 15g of a propellant such as N_2H_4), the detection limit of zinc in parts per million is $(1.36 \times 10^{-7})\ (10^{6})/15 = .009$ ppm. This detection limit could be improved several orders of magnitude by activating in a higher flux for a longer time and by counting for a longer period. However, one must be willing to pay the penalty of the increased times and/or increased cost.

Similar calculations for iron and chromium yield detection limits of close to 0.1 ppm for iron and 0.001 ppm for chromium. The low natural abundance of iron-58, (0.33%) is largely responsible for the detection sensitivity being less than that of zinc and chromium. Although zinc-64 has a high natural abundance, the low cross section of zinc-64 and long half life of zinc-65 are restricting factors. The detection sensitivity for chromium is high, in part due to the high cross section of chromium-50 (16 barns) and in part to the short half life of chromium-51 (27 days). Also, the detector efficiency for a 0.33 Mev gamma is higher than that for a 1.1 to 1.3 Mev gamma (about 30 compared to 15% in the system employed in this study).

The absolute detection limits for these and other metals is determined by the saturation activity attainable in accordance with equation (6). As noted above, the detection limit for iron by neutron activation analysis is about 0.1 ppm (10^{-6} g Fe in a 10 g sample) using the activity calculated from equation (7) for a 10 hour activation in a flux of 8×10^{12}. The ratio of equations (6) and (7) is given by $(1/\lambda)/t$, which is the activity at saturation compared to the activity at time t. For iron-59 this ratio is 156 assuming $t = 10$ hours, which means that the detection limit can be decreased by a factor of 156 by activating to saturation (several months would be required). The simplest method of decreasing the detection limit is to activate in a higher flux, and there is no problem in attaining a flux in some reactors two orders of magnitude higher (approaching 10^{15}) than the 8 x 10^{12} encountered in the WSU reactor. Thus the absolute detection limit for iron by neutron activation analysis would be approximately four orders of magnitude less than the 0.1 ppm mentioned above, or, 0.0001 ppm. This assumes activation to saturation in a flux of 8 x 10^{14} followed by a reasonably short counting time in the equipment used in this program. Longer counting times in more elaborate equipment would give even lower detection limits. Note that the above limit is the detection limit for activation analysis, not the detection limit at which commercially available iron-59 tracers can be counted. This would be even lower, because such tracers are prepared by activating isotopically pure Fe^{58}. (Fe^{58} occurs naturally to the extent of only 0.33% in elemental iron.) The detection limit would thus be a factor of 300 lower, or less than 0.0000001 ppm, for such a tracer. Tracers prepared in this way were used in Task 2 of this program.

4.0 EXPERIMENTAL SECTION

4.1 Task 1 - Thermal Neutron Activation Analysis

The purpose of Task 1 was to develop thermal neutron activation as a method of analyzing quantitatively for metals dissolved or dispersed in liquid propellants. For purposes of demonstration, the experimental effort was limited to the metals iron, zinc, and chromium and the propellants nitrogen tetroxide and hydrazine.

In theory one could calculate the amount of metal present in an activated propellant sample making use of equation (8). In practice, however, exact measurement of variables such as the counting efficiency of the detector and the thermal neutron flux in the reactor is difficult. Also the cross sections are not accurately known for some isotopes. Consequently, the analyses were made with the aid of standards as discussed in the following paragraphs.

4.1.1 Procedure

In general the analytical procedure consisted of five steps: (1) preparation of propellant samples; (2) preparation of standards; (3) activation; (4) counting; and (5) resolution of spectra.

4.1.1.1 Propellants

Both "wet" and "dry" analyses were performed. In the case of the wet analyses 10 grams of the liquid propellant was sealed in a quartz tube prior to activation. The N_2H_4 (MIL-P-26536C) was obtained from Olin Mathieson Co. and the N_2O_4 (MSC-PPD-2A) was obtained from Southwest Potash Corporation. The quartz tubes were sealed with the aid of an acetylene-oxygen torch after freezing the contents of the tubes in the presence of a stream of dry helium. The dry analyses were accomplished by activating the residue left after evaporating 10 grams of the propellant to dryness with the aid of a stream of dry nitrogen gas. Quartz, polypropylene, and polyethylene tubes were employed for the dry analyses.

4.1.1.2 Standards

Both wet and dry standards were prepared. It was necessary to have two sets of standards because the differences in geometrical distribution of the radioactive contaminants in the wet and dry cases result in slightly different counting efficiencies. In the dry case the radioactivity is concentrated in the bottom of the container tube. This places the sample deeper within the NaI detector well where more of the gammas can be captured, producing a somewhat higher count rate than in the case of the wet standards (see Table 2).

The calibration tubes consisted of 19 mm O.D. polypropylene, polyethylene, and quartz tubes. The quartz tubes were obtained from Engelhardt Inc. and the polypropylene and polyethylene tubes from Van Waters and Rogers (Cat. Nos. 60817-245 and 16448-081, respectively). Pure quartz and hydrocarbon plastics do not activate to give any interfering radiation. The silicon-30 in quartz activates to yield silicon-31, a gamma emitter (1.26 Mev), but the half life is so short (2.62 hours) that after a couple of days the radioisotope has decayed to negligible proportions. Light atoms such as hydrogen, carbon, nitrogen, and oxygen do not activate to any appreciable extent. Tritium ($_1H^3$) and carbon-14 are both beta emitters and are produced in such minute amounts that they are to be regarded as completely inconsequential.

Wet standards were prepared by adding to the polypropylene tubes aqueous solutions of four concentrations of each metal (1, 10, 100, and 1000 ppm). Reagent grade iron, zinc, and ammonium dichromate were employed as primary standards. The iron and zinc solutions were prepared by dissolving weighed amounts of the metals in a small amount of nitric acid and diluting the resulting metal nitrate solutions with enough water to give concentrations of 1000 ppm. Successive dilutions then yielded solutions of 100, 10, and 1 ppm. The ammonium dichromate was weighed out and dissolved directly in water to give the initial concentration of 1000 ppm. The substances ammonium dichromate, metallic iron, and metallic zinc were chosen in part because the other atoms introduced into the resulting solution (hydrogen, nitrogen, and oxygen) do not activate to give interfering gamma emissions. A complete set of standards (1000, 100, 10 and 1 ppm for each of the three metals) was made only in the case of the polypropylene tubes.

The dry standards were prepared by starting with a set of solutions identical to the wet standards, placing the tubes in a vacuum desiccator, and evaporating the contents to dryness. The water used for both the wet and dry standards was obtained from a Barnstead demineralizer using a mixed-bed type ion exchanger.

All tubes were hermetically sealed to prevent reactor water from leaking into the tubes. The quartz tubes were sealed with an acetylene-oxygen torch, and the plastic tubes were sealed by placing a tight fitting plastic cap in the mouth of the tube and fusing the two together with a hot glass rod.

4.1.1.3 Facilities and Equipment

The activation was performed in the Washington State University reactor. The irradiation was carried out for 10.87 hours at a thermal neutron flux of about 8×10^{12} neutrons per cm^2 per sec. The cadmium ratio (the ratio of thermal neutrons to fast neutrons) was 10 and the gamma dose rate was about 5×10^7 rads per hour.

The reactor is of the swimming pool type. The samples were loaded into four 2 7/8" x 20" irradiation tubes which were adjacent to the core of the reactor. The tubes were of such a size to accommodate the presence of three bundles of six standards per tube. The three bundles were stacked on top of one another. These tubes were rotated during the irradiation period to insure a uniform flux. Iron wires (five inches long, 0.009 inch diameter) were placed in each bundle of standards so that the flux could be measured. The different bundles of samples and standards could then be related to one another even though each might have been exposed to a slightly different flux.

The gamma counting was accomplished with a 3" by 3" sodium iodide scintillation detector with 1" x 1 1/2" well (Harshaw Company). The multiple phototube output was amplified by a charge sensitive preamplifier of Boeing's own design followed by a Technical Measurements Model CN 1024 multi-channel analyzer with a tabular printout.

4.1.1.4 Gamma Counting and Spectra Resolution

The final step in the analytical procedure was to count the activated propellant samples and compare the count rates corresponding to Fe^{59}, Zn^{65}, and Cr^{51} with those of the standards. This is a simple matter if only one component (e.g., Zn^{65}) is present. If several components are present (e.g., Fe^{59}, Zn^{65}, Cr^{51}, and other metal impurities such as Cu^{66} and Co^{60}), then the different spectra overlap one another and must be resolved.

Figure 2 shows spectra of Cr^{51}, Zn^{65}, Fe^{59}, and their sum. If, for example, only Zn^{65} were present, then one would simply determine the area (count rate) under the 1.12 Mev peak (perhaps in the energy range 1.02 to 1.22 Mev) and match this area (corrected for background) to the area of a standard. If, however, Fe^{59} were also present, the count due to the 1.10 Mev peak of Fe^{59} would cause considerable interference as shown in the sum curve of Figure 2. There is also background interference from the 1.29 Mev peak of iron.

This background is due largely to Compton scattering, which causes a peak to tail at the low energy side. This tailing derives its origin from scattering of the gammas (which are emitted at a discrete energy) by electrons which produces a successive reduction in energy of a fraction of the gammas.

One method of resolution which was successfully employed in this program was the progressive subtraction of standard spectra of iron, zinc, and chromium. To illustrate this process consider Figure 2. Referring to the sum spectrum, one can see that there are three major peaks: the first at 0.32 Mev due to Cr plus background from Fe and Zn; the second at about 1.1 Mev due to the sum of the 1.10 Mev peak of Fe, the 1.12 Mev peak of Zn, and background from the 1.29 Mev peak of Fe; and the third at about 1.3 Mev, due almost entirely to Fe. The resolution process consisted of subtracting a standard Zn spectrum (within the multichannel analyzer unit) until the ratio of the areas (or, more simply, the heights) of the peaks at 1.1 and 1.3 Mev was equal to the ratio of the areas (or heights) of the 1.10 and 1.29 Mev peaks of pure Fe. A standard Fe spectrum was then subtracted until the peaks at 1.1 and 1.3 Mev disappeared; only the Cr peak at 0.32 Mev then remained.

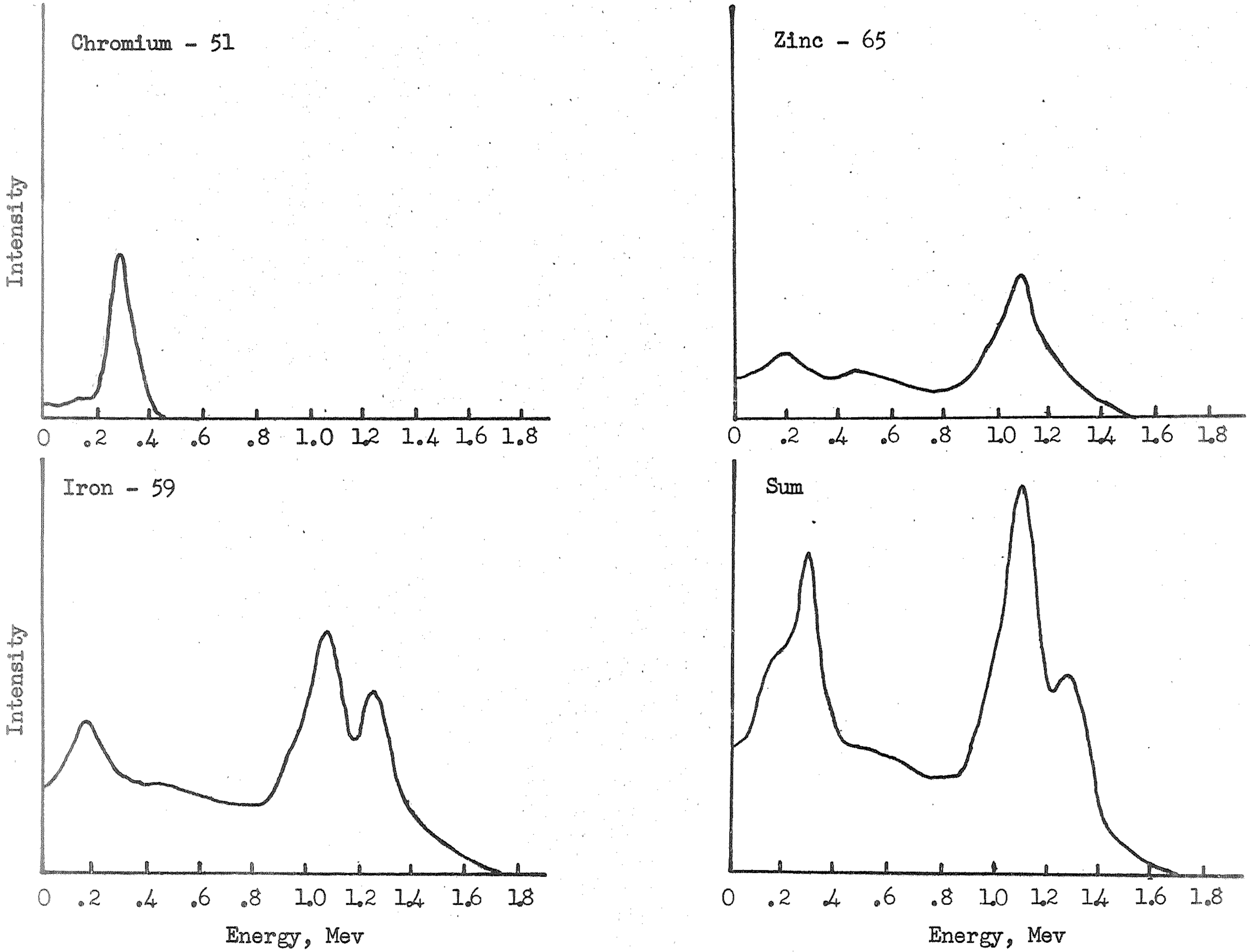

Figure 2: GAMMA SPECTRA OF CHROMIUM - 51, ZINC - 65, IRON - 59, AND THEIR SUM

This subtraction process is easily done, but can become tedious if many spectra must be analyzed. Consequently, this contractual effort made use of the SHIFTY III computer program, a linear least squares fitting program for the isotopic analysis of gamma ray spectra.

4.1.2 Results and Discussion of Task 1

4.1.2.1 Standards

The irradiation of the standards was successfully accomplished, although all three container materials contained traces of elements which activated to give interfering gamma spectra. Furthermore, polypropylene underwent significant radiation damage, causing two of the tubes to become brittle and crack. These and other results are summarized in Table 1.

TABLE 1. Comparison of Container Materials

Material	Comments
Polyethylene	In general, the best material tested. No significant radiation damage and a low background (comparable to natural background).
Polypropylene	Marginal as a container material. Appreciable radiation damage (tubes became brittle) with background about 10 times that of polyethylene.
Quartz	Although radiation damage was not a factor, impurities in the quartz activated to produce a very high background (about 100 times that of polyethylene.)

The only impurities positively identified were sodium in both polyethylene and polypropylene and zinc in quartz. There were various short lived isotopes present that decayed away in a matter of a day or two and longer lived isotopes such as sodium-24 (half life, 15 hours) that were gone in a week's time. However, there were longer lived isotopes present whose activity still persisted after one week. Major gamma peaks after one week's decay were found at the following energies (in Mev): polyethylene, 0.40 (half life, about 70 hours);

polypropylene, 0.40 (half life, about 30 hours), 0.56 (half life, about 30 hours); quartz, 1.12 Mev (due to zinc).

Table 1 indicates that the backgrounds of the polypropylene and quartz tubes were respectively one and two orders of magnitude higher than the polyethylene tubes. Since the method of manufacture of the tubes can strongly affect the impurity content, the above background levels should not be considered typical of polyethylene, polypropylene, and quartz in general, but rather the values for these specific tubes.

To avoid correcting for the background of the tubes, the contents were simply transferred to unactivated 19 mm glass test tubes. In the case of the dry standards, the precipitate in the bottom of the tube was simply redissolved in 10 grams of water before transferring to the test tube. The resulting solution was then used as a wet standard or re-evaporated to the dry state as desired.

A special difficulty was encountered with the wet chromium standards. After irradiation a green precipitate was noted in the bottom of the tubes. The precipitate was not identified, but the color was suggestive of a Cr (III) compound. It is possible that radiation in the reactor induced reduction of the $(NH_4)_2 Cr_2O_7$ to a Cr (III) compound. The presence of a precipitate in the bottom of the tube is objectionable, because the geometrical distribution of the Cr^{51} atoms would be closer to that of a dry standard.

The wet standards were used to check the linearity of the detector as a function of count rate. Figure 3 shows a plot of count rate versus metal concentration for those standards for which data were available. As can be seen, there were no deviations from linearity. This means that only one standard at any concentration would be sufficient to perform analyses of propellants containing metals whose concentration varied over many orders of magnitude.

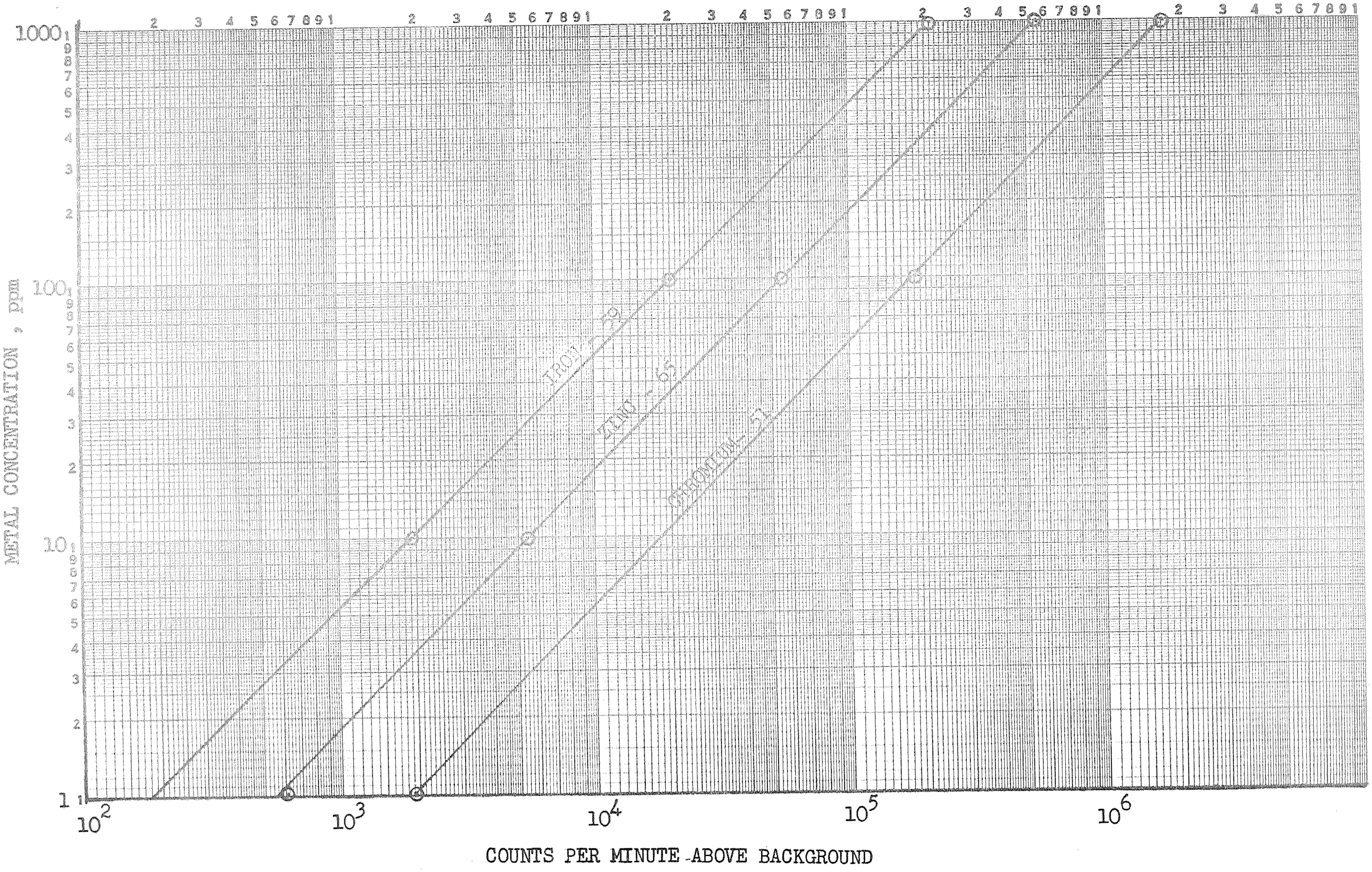

FIGURE 3: RADIOACTIVE METAL CONCENTRATION AS A FUNCTION OF COUNT RATE

The standards were also used to compare the count rate relationship between the wet and dry state. Table 2 shows that in general the count rate for the dry standards was about 30% greater than the count rate for the wet standards. This inequality is explained by different counting efficiencies which arise from the different geometrical distributions of the radioactive atoms. Absorption of gammas by the water of the wet standards is almost negligible and would not contribute to the inequality in count rate. The table includes all wet-dry pairs for which a comparison could be made. A few samples were ruined during the irradiation process because of leakage of water into or out of the tubes and for some samples the background of the polypropylene tubes interfered too much. The two members of any wet-dry pair were counted for equal times such that about 50,000 counts were recorded for each pair. The counts were corrected for flux (see Section 4.1.2.3).

TABLE 2. Comparison of Wet and Dry Standards

Standard	State	Counts (corrected for flux)	Count Ratio (dry/wet)
1000 ppm Fe	dry	58,000	1.37
"	wet	42,180	
100 ppm Zn	dry	54,950	1.26
"	wet	43,500	
10 ppm Zn	dry	58,500	1.38
"	wet	42,000	
1000 ppm Cr	dry	49,770	1.15
"	wet	43,000	
100 ppm Cr	dry	77,610	1.36
"	wet	57,200	

There is some uncertainty in the exact relationship between the wet and dry count rate, since one of the sources of error of the dry method is associated with the lack of reproducibility of residue deposition during the evaporation process. Minor variations in distribution of the radioactive residue will occur from tube to tube, and the detector, which is quite sensitive to such geometrical differences, will record varying count rates. The relatively large spread in ratios (1.15 to 1.38) is indicative of these geometrical differences.

4.1.2.2 Propellant Analysis

In addition to the activation analysis study, analyses of the specification grade propellants were made by conventional means. Table 3 summarizes the results. Analyses for metals were made with a Perkin-Elmer Model 303 atomic absorption spectrometer.

TABLE 3. Characterization of Propellants

MSC-PPD-2A N_2O_4

Constituent	Spec Limits	Found
N_2O_4, %	98.65 min	99.04
NO,%	0.65 ± 0.2	0.80
H_2O equivalent, %	0.1 max	0.01
NOCl, %	0.08 max	trace
Fe, ppm	not required	0.7
Zn, ppm	not required	< 0.1
Cr, ppm	not required	< 0.1

MIL- P-26536C N_2H_4

Constituent	Spec Limits	Found
N_2H_4, %	97.5 min	98.3
H_2O, %	2.5 max	0.065
particulate	10.0 max	0.2
Fe, ppm	not required	< 0.2
Zn, ppm	not required	< 0.1
Cr, ppm	not required	< 0.2
Cu, ppm	not required	< 0.1

The N_2H_4 was sampled from the middle of the 50 gallon drum prior to the activation analysis study. The N_2O_4 used for the metals analysis was also sampled prior to the activation analysis study and was taken from the upper one third of the storage tank (initially containing about 350 lb. of propellant).

The N_2O_4 used for the remainder of the analysis of Table 3 was drawn from the bottom of the tank after about 80-90% of the N_2O_4 had been removed and used during Task 2. An iron analysis by atomic absorption at this time yielded a value of 0.35 ppm, half of the iron content at the start of the program.

The analyses are noteworthy for the low concentrations of metals present in the two propellants. Other workers have reported concentrations that average about an order of magnitude higher.[2,4] Iron in N_2O_4 (0.35 to 0.7 ppm) was the only metal that was present in measurable quantity. All other metals were present in concentrations below the detection limit of the instrument. However, even the iron concentration was relatively small, since values greater than 1 ppm are usually reported.

By activation analysis the dry N_2O_4 samples yielded a value of 0.4 ppm iron. This is acceptable agreement with the atomic absorption results, especially in view of the fact that the range of iron concentrations (0.35 to 0.7 ppm) measured by atomic absorption suggests that the results of the analysis may be quite sensitive to the time and manner of sampling.

It seems very possible that the iron concentration in a storage tank varies as a function of depth. Iron compounds in suspension would tend to settle with time (assuming the particle size is large enough). Thus the iron concentration at the bottom of the tank would be greater than that at the top of the tank. The fact that by atomic absorption the value (0.7 ppm Fe) found in the N_2O_4 taken from the top third of the tank was higher than that taken from the bottom of the tank (0.35 ppm Fe) is explained by the sampling sequence. The lower value was obtained after most of the N_2O_4 (80-90%) had been siphoned off for use in Task 2. Since the siphon tube extended close to the bottom of the tank, the first N_2O_4 withdrawn was probably richer in iron than the last portion of N_2O_4 removed. Continued settling and further N_2O_4 removal reduced the iron content with time until relatively little remained in the final 10-20%.

The dry analytical method could not detect zinc or chromium in N_2O_4 and none of the three metals in N_2H_4. The detection limits are about 0.1 ppm for Fe, 0.01 ppm for Zn, and 0.001 ppm for Cr. Thus reasonably good agreement was obtained between activation analysis and atomic absorption analysis, which also was unable to detect these elements.

Activation analysis employing the wet analytical technique was unsuccessful with both propellants, but for different reasons. In the case of N_2H_4, the quartz tube containing the fuel exploded at some time during the course of the irradiation. The tube was practically pulverized by the violence of the explosion. Efforts had been taken to reduce the chances of such an occurrence. A sizeable helium-filled ullage volume (10 cc) was present in the tube. The temperature rise was expected to be small, since the outer aluminum container (in which the quartz tube was packed) was immersed in circulating reactor water whose temperature probably did not exceed 90°F. The explosion can be satisfactorily explained by gamma-induced decomposition of the N_2H_4. This possibility was considered prior to the irradiation, and using decomposition rate data in the literature[5,6] and a dose rate of 10^6 rads per hour, the pressure increase due to decomposition was calculated to be only one atmosphere for a 10-hour irradiation. The dose rate of 10^6 rads per hour was the best available estimate at the time the calculations were made, but subsequent to the irradiation it was learned that the dose rate was 50 times higher (5×10^7 rads per hour). This would produce a pressure increase of 50 atmospheres, more than enough to burst the quartz container. It should be noted that N_2O_4 would undergo an insignificant amount of radiation-induced decomposition under identical conditions.[5,6]

In the case of the wet N_2O_4 analysis, an unexpectedly high level of radioactivity was found in the propellant (after transferring the contents from the activated quartz container to an unactivated glass container to minimize background effects). This level of radioactivity was so high that the presence of any iron, zinc, or chromium would have been masked.

When the N_2O_4 was vacuum distilled, practically all of the radioactivity distilled with the N_2O_4. A determination of the half life of the volatile radioactive contaminant yielded a value of 35 hours. A survey of gamma emitters of half life close to 35 hours led to the identification of bromine-82 (half life, 35.9 hours) whose literature spectrum singularly fit the spectrum of the volatile impurity. The amount of bromine present could not be accurately estimated in the absence of bromine standards, but a concentration of close to 100 ppm would be required to give such a strong spectrum. The bromine most likely owed its origin to the N_2O_4 preparative method, which involved the reaction of KCl with HNO_3. KBr was present as an impurity in the KCl.*

4.1.2.3 Errors

Sources of error in activation analysis have been the subject of considerable study and have been thoroughly discussed elsewhere.[7] The proper use of standards tends to reduce or eliminate errors by cancellation; that is, both the sample and standard are exposed to the same activation conditions.

A possible problem arises when the sample and standards are not exposed to exactly the same environment in the reactor. An error will obviously occur if, because of a non-uniform flux distribution in the irradiation tube, the sample and standard receive different fluxes. In this study this problem was obviated in part by the rotation of the irradiation tubes at the Washington State University reactor. However, there was a variation in flux along the length of the tubes, reaching maximum intensity in the middle and having the minimum values at the two ends. As explained in Section 4.1.1.3, each bundle of standards or propellant samples contained a five inch long iron wire so that flux variations could be measured. After the activation was complete, the wires were cut into four 1/2 inch segments and counted. The average flux received over these four segments could then be calculated.

Figure 4 shows the flux distribution in three bundles of standards stacked on top of each other in one of the irradiation tubes. The three iron wires were labeled 6, 7, and 8. Number 6 was on the bottom, 7 in the middle and 8 on top. As expected, the minimum fluxes were found at the bottom of wire 6 (about 8 x 10^{12})

---

* Private communication with Nolan Dodin, Southwest Potash Corporation.

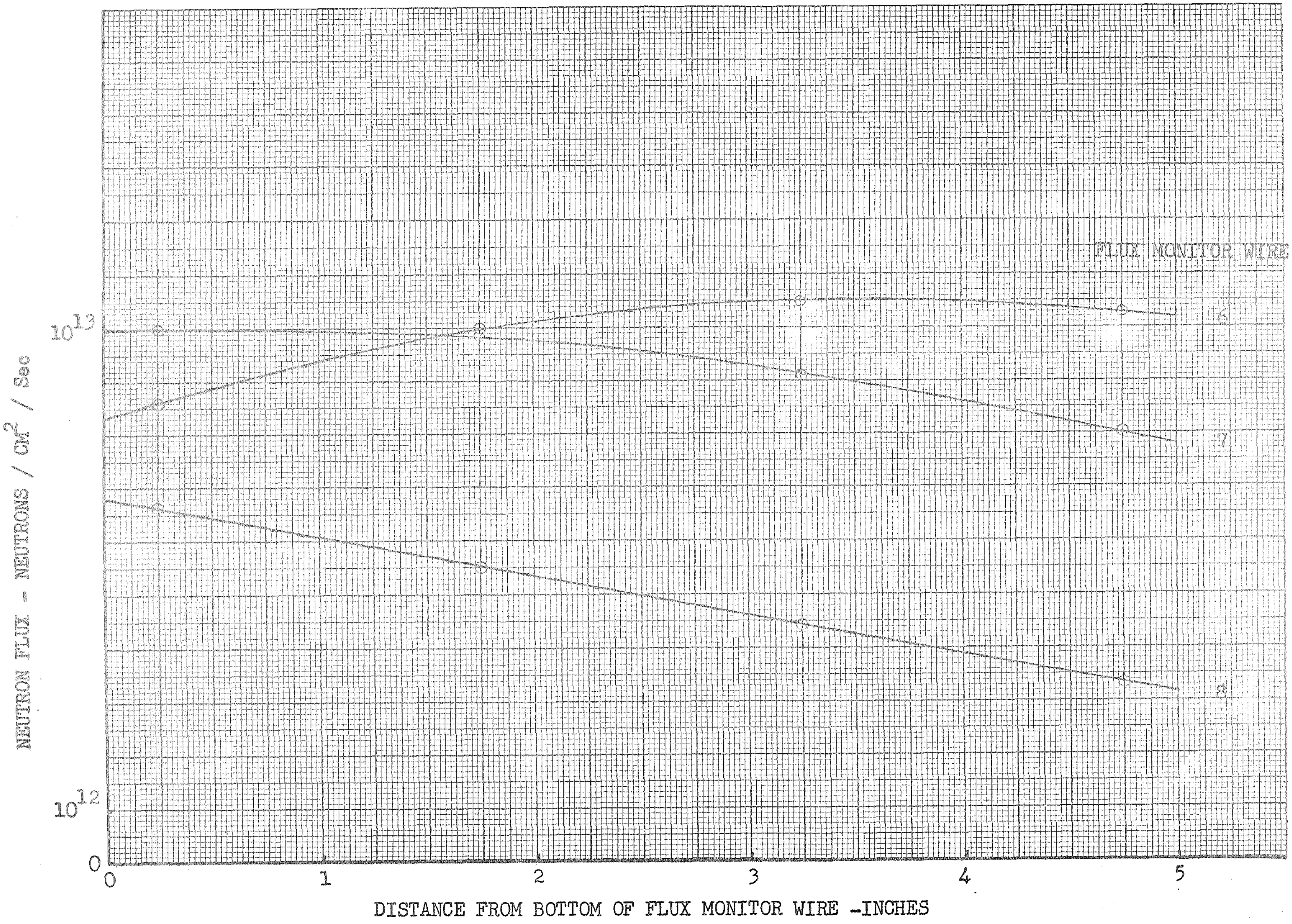

FIGURE 4: NEUTRON FLUX DISTRIBUTION

and the top of wire 8 (about 2 x 10^{12}). The flux increased up wire 6, reaching a maximum slightly in excess of 10^{13} near the top of wire 6. The bottom of wire 7 picked up the flux at about 10^{13} and declined along the wire reaching 7 x 10^{12} at the top of the wire. Because of small spaces between the bottom and top of wires 6 and 7 and wires 7 and 8, the flux value of an adjacent wire did not start exactly where the other left off. Thus the bottom of wire 8 began at about 6 x 10^{12} instead of 7 x 10^{12}, the value at the top of wire 7.

The data of Figure 4 allow one to normalize two samples exposed to different total fluxes anywhere within the irradiation tube simply by making a flux correction. In this program an effort was made to put the propellant samples side by side with the standards so that no longitudinal flux correction had to be made.

4.1.2.4 Spectra Resolution

In Section 4.1.1.4 the method of spectra resolution by progressive subtraction was explained. Although this could be done manually, a faster and more elegant method was through the use of the SHIFTY III computer program. The question of relative worth of the computer program turned out to be rather academic, since none of the propellant samples yielded any spectra that had to be resolved.

Before performing the propellant activation, a check was made on whether a simultaneous analysis of Fe^{59}, Zn^{65}, and Cr^{51} could be successfully accomplished. This was done by preparing and analyzing an aqueous solution containing these three radioisotopes. The metal activities corresponded to those that would result from the 10 hour activation at the WSU reactor of 10 grams of propellant containing 2 ppm Fe, 0.2 ppm Zn, and 0.01 ppm Cr. When the spectrum of the mixture was resolved by the manual progressive subtraction of standard spetra of Fe^{59}, Zn^{65}, and Cr^{51}, the concentrations that were found were 1.7 ppm Fe, 0.21 ppm Zn, and 0.011 ppm Cr. Thus the values were about 15% low for iron, 5% high for zinc, and 10% high for chromium. This is good agreement considering the low activities (concentrations) involved.

It was expected that the computer program might perform a somewhat more accurate analysis. However, the computer program yielded the same results.

It would seem that although the propellant samples yielded no spectra to be resolved, the above analysis of the laboratory "unknown" indicates that spectra resolution is not a problem area.

4.2 Task 2 - Propellant Flow Tests

The main purpose of Task 2 was to demonstrate that radioactive tracers are capable of serving as a highly sensitive tool for diagnosing flow decay problems. In its simplest form the tool would consist of a detector which would externally scan various parts of a feed system and check for contaminant deposition (gamma emissions) at those parts. Because of the great sensitivity of the technique, contaminant deposition could be detected in advance of the time at which a clogging problem would be discernable by conventional methods.

Flow tests were conducted with both N_2O_4 and N_2H_4. The first tests of this program were made on N_2O_4, since its clogging behavior is better established[1,2,4,8, 9, 10] than that of N_2H_4.[4, 11.] Testing of N_2H_4 proceeded after sufficient knowledge had been gained on how to apply the tracer technique to N_2O_4. In order to make reasonable comparisons with previous results, test conditions and test equipment were similar to those of previous studies.[2,4]

Prior to beginning the tests consideration had to be given to the means of introducing radioactivity into the propellant. The four possible methods are listed in Table 4.

Method A, direct activation of the propellant and its metal contaminants is ideally the best, since the chemical and physical states of the metal compounds in solution (or suspension) are probably not altered by the activation process. The main disadvantage is that only small quantities of propellant can be activated because of space limitations in a reactor. Method B, which involves activation of the residue left after evaporation of the propellant followed by redissolving the residue, allows large quantities of propellant to be used, but the evaporation

TABLE 4. Methods of Introducing Radioactivity into Propellants

A. Activate liquid propellant

1. Advantage - The chemical and physical states of the propellant contaminants (metal compounds) are not altered.

2. Disadvantage - Because of limited reactor space only small quantities of propellant can be activated.

B. Activate residue left after evaporation of propellant and then redissolve residue in propellant

1. Advantage - Large quantities of propellants can be handled.

2. Disadvantage - Evaporation may change the chemical and/or physical state of the metal contaminants.

C. Add radioactive tracer to propellant

1. Advantage - Simplicity and high sensitivity.

2. Disadvantage - The chemical and physical state of the radioactive tracer may be different from that of the metal contaminants in solution.

D. Allow radioactive metal foils to interact with high purity (initially metal-free propellant

1. Advantage - Since metal contaminants will be formed in the proper chemical and physical state, one can duplicate the build-up of metal contaminants over any desired storage period.

2. Disadvantage - Long aging periods may be required.

process may change the chemical and physical states of the contaminants. Maintaining the proper chemical and physical state is important, since the mechanism of flow decay may depend strongly on the chemical and physical state of the metal contaminants.

Method C, the direct addition of a radioactive tracer to the propellant, was employed extensively in this program. This method has the advantages of unusually high sensitivity as well as simplicity. The very high sensitivity results from the fact that many radioisotopes having high specific activities (the ratio of radioactive atoms to total atoms) can be purchased from commercial sources. The specific activity is higher than that attainable by ordinary activation, because commercial sources can make use of such procedures as isotopic enrichment and/or very long activation times to yield high specific activities. In many of the runs as little as 10^{-5} gram of iron, zinc, or chromium (as solutions of the chloride or nitrate) was added to 2 gallons of propellant (about 0.001 ppm), and this quantity of material produced a very high count rate of the order of 1,000,000 cpm when only about 1% of the radioactive contaminants deposited in the test section. The main disadvantage of Method C is that one cannot be completely certain that the tracer compound takes the same chemical and physical form of the corresponding metal compound contaminant that is naturally present in the propellant. It does, however, seem quite possible, if not in fact likely, that through intermolecular exchange or other chemical equilibration process the tracer will be transformed into the proper state. This would be particularly true if the tracer were added in a chemical form that is known to approximate that of the metal in solution. For example, in the N_2O_4 tests of this program, Fe^{59} was usually added as $Fe(NO_3)_3$ dissolved in a small amount of concentrated nitric acid, a chemical form not too different from that of the ferric nitrate complexes that have been reported in flow decay deposits ($Fe(NO_3)_3:N_2O_4$ and $Fe(NO_3)_3 \cdot 9H_2O$).

Method D received some attention in this program. A major advantage is that this method can be used to determine whether flow decay is likely to occur after a long term aging period. In the case where an equilibrium metal concentration (for example, a solubility limit) is reached after a long interaction time in a propellant storage tank, the same metal concentration can be duplicated in the laboratory in a shorter time by increasing the surface area of the radioactive foil, so that the rate of dissolution is accelerated.

4.2.1 Equipment

A schematic representation of the test system is shown in Figure 5. All valves were operated manually. The valves, tanks, fittings, and fluid lines (1/4 inch O.D.) were of 304, 316, or 321 stainless steel. For easy installation and removal, the feed and catch tanks were connected to the fluid line with a short piece of Aeroquip 666 Teflon hose. All O-rings were of either Teflon or Parker compound B591-8. Drilube, Type 882, was used where a thread lubricant was needed.

For the tests involving filters, the feed and catch tanks were of 2.3 gallons capacity. The tanks were flanged at the top to permit access to the interior for cleaning. Each tank was equipped with a pressure gauge and fill, vent, and drain valves. In addition, the feed tank had a dip tube outlet, a sight gauge, and a relief valve. The seal between the flanges was a tongue-in-groove flat Teflon gasket type.

In the case of the capillary tests, a smaller (250 cc) feed tank was required because of the much lower flow rates. Its dimensions (about 1 inch diameter by 20 inches tall) were such that a long sight gauge could be attached to the tank so that flow rate measurements could be taken with the aid of graduated marks along the sight gauge.

Figure 5 also shows the location of pressure and temperature sensing devices. Pressure transducers and thermocouples were employed to continuously monitor the pressure and temperature at key locations in the test system. The heat exchanger pictured in Figure 5 was a 20 foot coil of tubing submerged in a

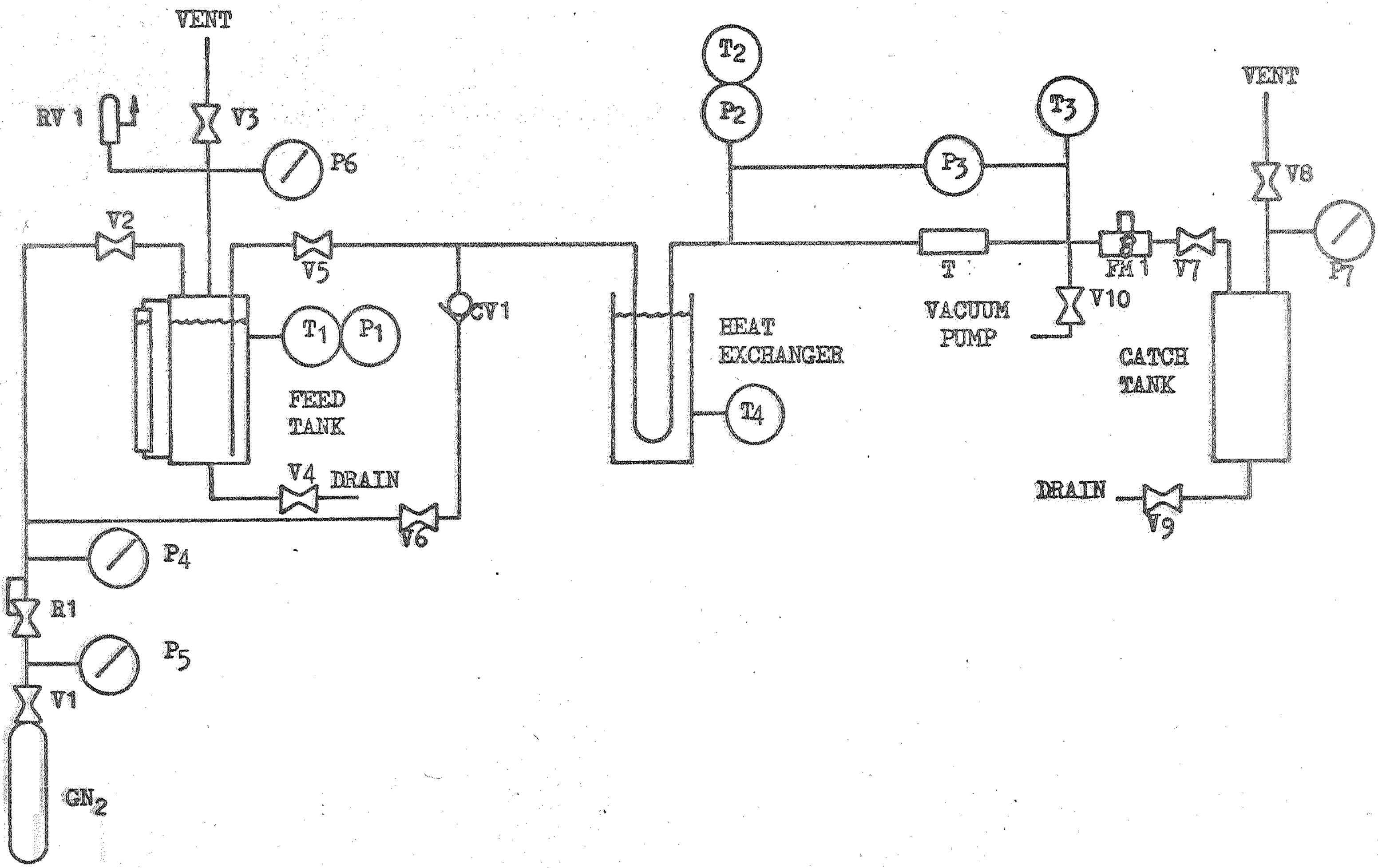

FIGURE 5. SCHEMATIC REPRESENTATION OF TEST ASSEMBLY

CALC

CHECK

APPD

APPD

REVISED

DATE

HARDWARE LIST FOR FIGURE 5

THE BOEING COMPANY

PAGE

SYMBOL	DESCRIPTION	SIZE	TYPE	SERVICE	REMARKS
V 1	N_2 Cylinder Shutoff	-			On cylinder
V 2	N_2 Pressurization Shutoff	½" JB			
V 3	Feed Tank Vent	½" JB			
V 4	Feed Tank Drain	½" JB			
V 5	Feed Tank Flow Control	¼" Grove			
V 6	Purge Shutoff	¼" Grove			
V 7	Catch Tank Inlet	¼" Grove			
V 8	Catch Tank Vent	½" JB			
V 9	Catch Tank Drain	½" JB			
R 1	GN_2 Regulator	0-100 PSIG			
T	Test Section				Filter, Capillary Tube, or both.
CV 1	Purge Check Valve	½"	Poppet		Circle Seal
RV 1	Feed Tank Relief	½"	Poppet		Circle Seal
V 10	Vacuum Pump Shutoff	½"	JB		

INSTRUMENT LIST FOR FIGURE 5

THE BOEING COMPANY

CALC	CHECK	APPD	APPD

REVISED

DATE

PAGE

SYMBOL	DESCRIPTION	ACCURACY	DATA RANGE	REMARKS
P 1	Feed Tank Pressure	± 2%	0-100 psig	
P 2	Test Section Inlet Press.	± 2%	0-100 psig	
P 3	Test Section Diff. Press.	± 2%	10 to 40 psid	
P 4	R 1 Outlet Press.	± 10%	0-200 psig	Regulator Gauge
P 5	R 1 Inlet Pressure	± 10%	0-3500 psig	Regulator Gauge
P 6	Feed Tank Pressure	± 10%	0-100 psig	Gauge
P 7	Catch Tank Pressure	± 10%	0-100 psig	Gauge
T 1	Feed Tank Temp.	± 2%	50° to 110°F.	
T 2	Test Section Inlet Temp.	± 2%	32° to 70°F.	
T 3	Test Section Outlet Temp.	± 2%	32° to 70°F.	
T 4	Heat Exchanger Bath Temp.	± 5%	32° to 110°F.	Glass-Mercury Thermometer
FM-1	Flow Rate	± 2%	.1 to 1.0 GPM	

constant temperature bath. The flow meter used in the first seven runs was a Fischer-Porter turbine type flow meter (Model 1061505). In subsequent runs an orifice plate flow meter was employed.

Radioactivity was measured with a 3" x 3" right cylindrical NaI crystal detector in close proximity to the test section. The pulses of light, produced in the crystal by incident gamma rays, were detected by a photomultiplier tube and were analyzed and counted with a Baird Atomic Model CS202 dual channel analyzer, two Model CS127 scalers and one Model CS107 scaler, and a CS905 timer. The three scalers recorded counts in the energy intervals characteristic of radioactive Cr^{51}, Zn^{65}, and Fe^{59} respectively.

The test section contained either a filter or a capillary. The 10 micron absolute stainless steel filters were of wire mesh construction (Western Filter Co., Inc., part number S12-19310-2). Bubble tests made on eight filters selected at random gave absolute micron ratings in a range of 9.6 to 10.8 microns. Three 10 inch long capillaries were used in the tests. Two were 8 mil I.D. of type 304 stainless steel and one was 13 mil I.D. of type 321 stainless steel.

Figures 6 and 7 show the filter test sections. A glass housing (Figure 6) made from a Corning Pyrex pipe reducer was used in the first five tests. The glass housing permitted visual observation of any matter that might have deposited on the filter. In subsequent runs, the filter was enclosed by standard stainless steel fittings (Figure 7). The holes drilled in the fittings in Figure 7 were to allow entry to the thermocouples. The metal fittings were somewhat more convenient in that the detector could be placed closer to the filter, permitting a higher counting efficiency and higher sensitivity. Although steel absorbs gammas to a greater extent than glass, the difference was inconsequential in the case of the two housings because the thicknesses of the glass and steel were such that only small fractions of the gammas were absorbed. The high penetrability of gammas was illustrated at one point in this program by finding only a 20% decrease in count rate when an iron-59 source was counted through a 1/4 inch thick steel plate.

NASA TULALIP 10M FILTER TEST
SEC. & SETUP - RADIOACTIVE TRACER
TECH. TO DETERMINE FLOW DECAY.
10-5-70

2A295571

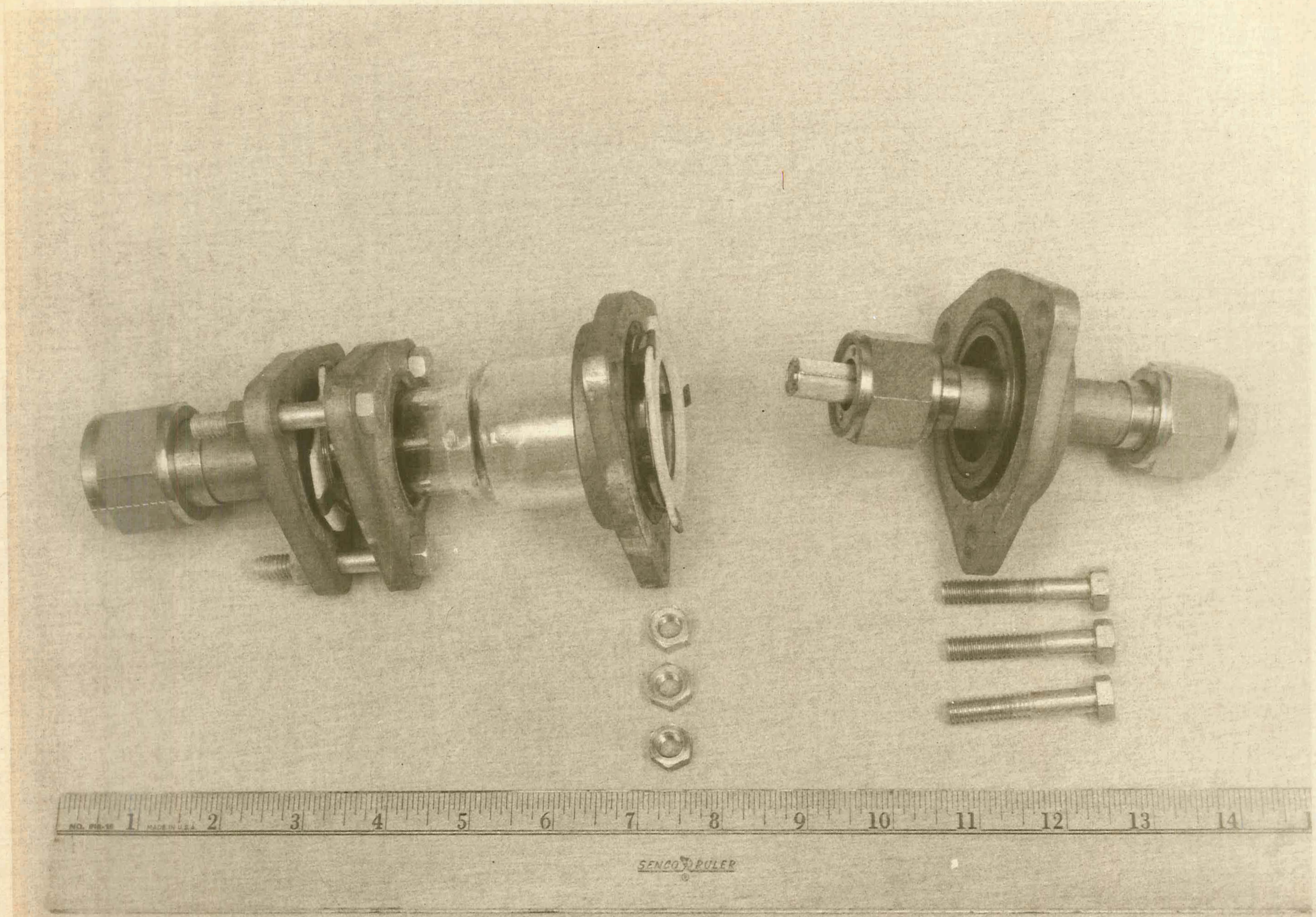

Figure 6: FILTER TEST SECTION (GLASS HOUSING)

NASA TULALIP - 10M FILTER TEST
SEC. & SETUP - RADIOACTIVE TRACER
TECH. TO DETERMINE FLOW DECAY.
10-5-70

2A295572

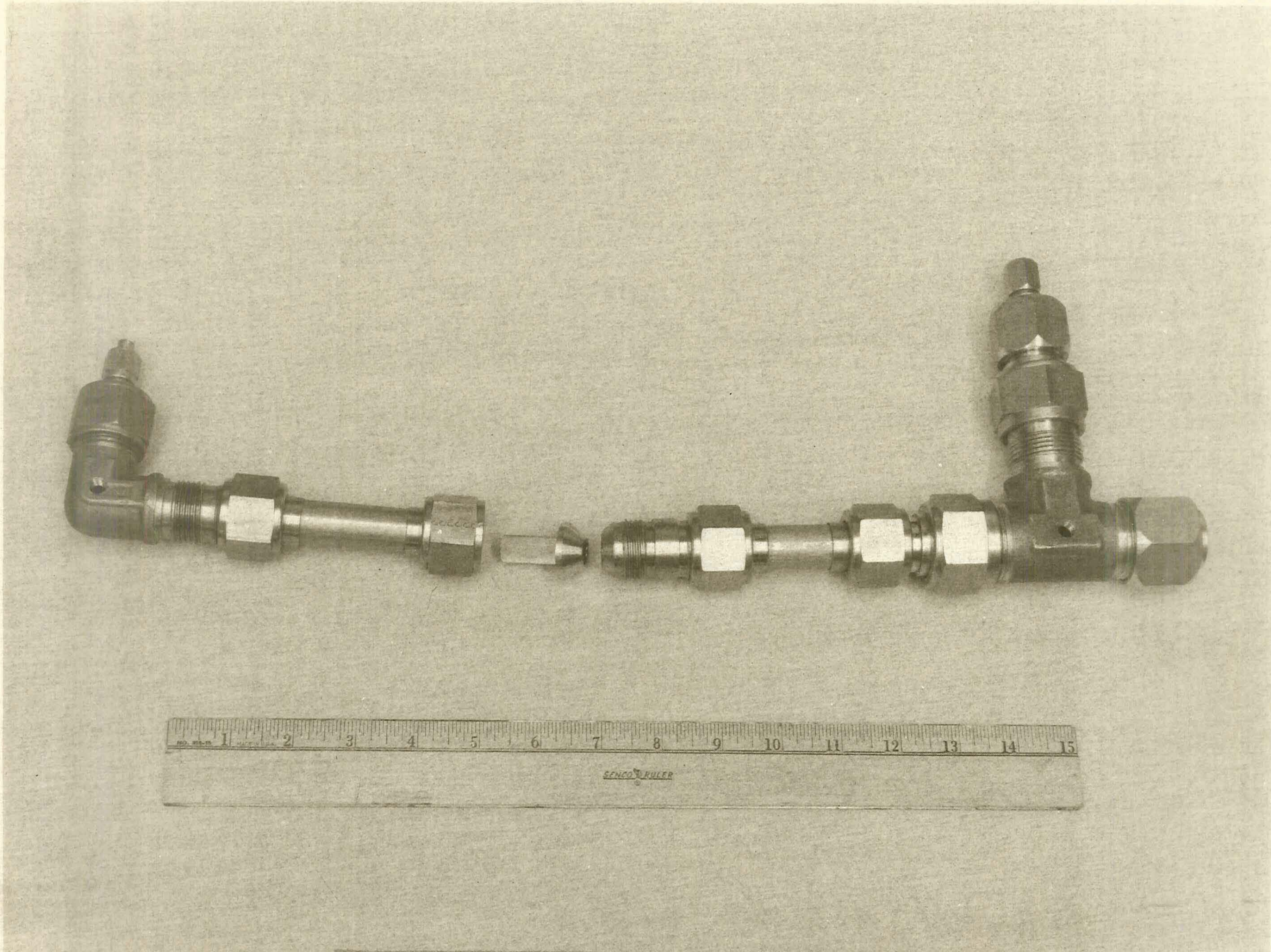

Figure 7: FILTER TEST SECTION (STAINLESS STEEL HOUSING)

Figure 8 shows a photograph of the apparatus used for a filter test. The feed and catch tanks were to the right and left, respectively, in the picture. The detector (not shown) was placed inside of the shielding cave formed by the 2" x 4" x 8" lead bricks. The test section is located in front of the opening of the shielding cave.

Figure 9 shows a photograph of the appratus used for a capillary test. The capillary is in the foreground resting on top of the lead bricks. The 250 cc feed tank and its sight gauge are located to the right of the capillary. The two large tanks at the left of the photograph were used as catch and supply tanks for the capillary tests.

Figure 10 shows the nuclear detector in place for a capillary test. The detector is shielded with 2" x 4" x 8" lead bricks. The capillary can be seen to the left of the shielding bricks. The capillary rests in a groove in an aluminum plate. The groove allowed the detector to slide easily along the capillary so that radioactive contaminants could be detected as a function of length within the capillary.

4.2.2 Procedure

A flow test consisted of four principal steps: (1) cleaning of the components; (2) addition of the propellant to the feed tank; (3) introduction of radioactivity into the propellant; and (4) flow of the propellant through the test section.

4.2.2.1 Cleaning

The propellant tanks were cleaned before each run. Lines and valves were cleaned on an intermittent basis (e.g., when changing propellants or before a run involving distilled N_2O_4. The cleaning process consisted of three immersions (at 140°F for 1/2 hour) and three rinsings with deionized water between the immersions. The first immersion was in trichloroethylene. After

NASA - 10M FILTER TEST SETUP 2A296241
RADIOACTIVE TRACER TECH. TO DETERMINE
FLOW DECAY. 11-11-70

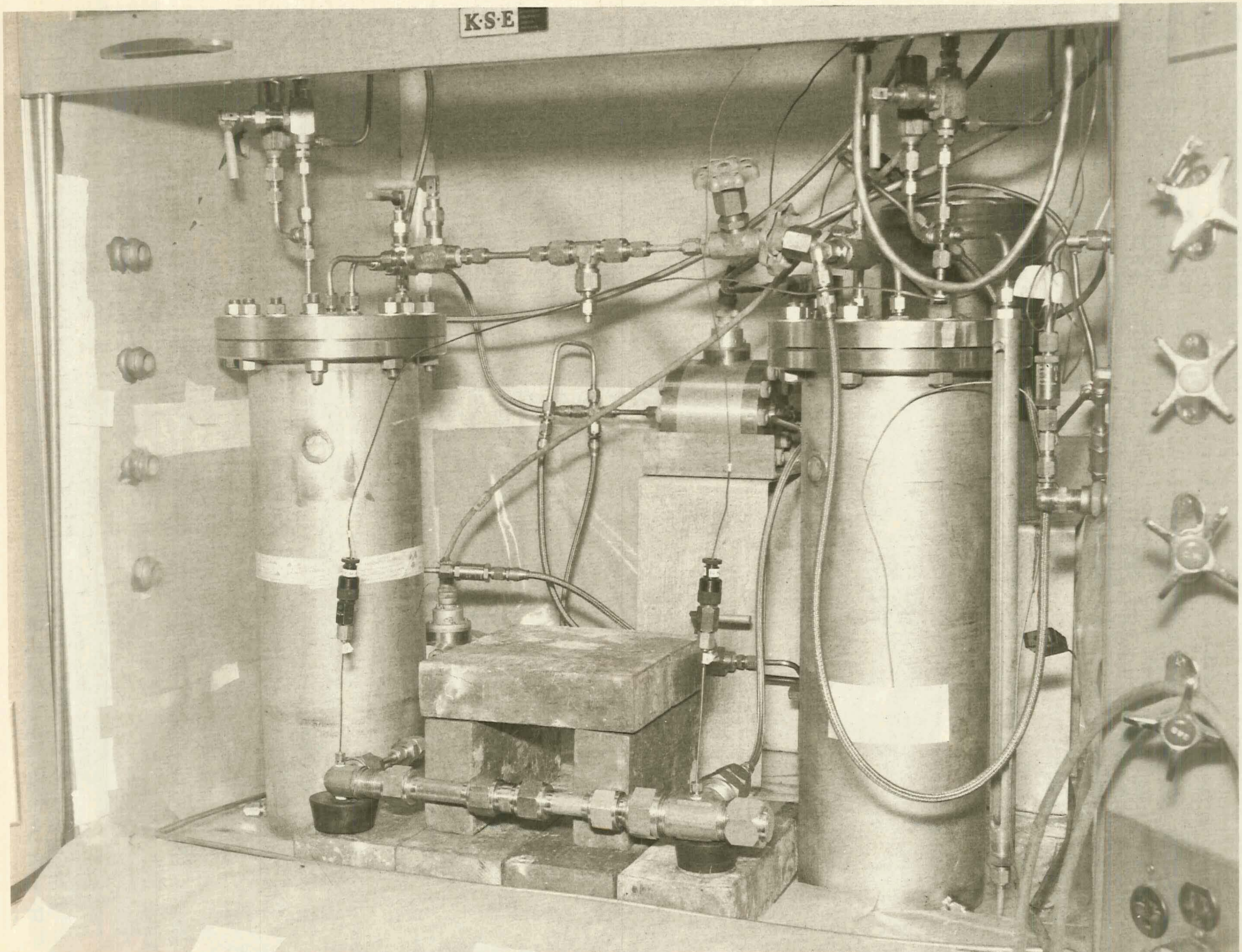

Figure 8: GENERAL VIEW OF THE FILTER TEST APPARATUS

[illegible]
NASA TULALIP - 10M FILTER TEST
SEC. & SETUP - RADIOACTIVE TRACER
TECH. TO DETERMINE FLOW DECAY.
10-5-70

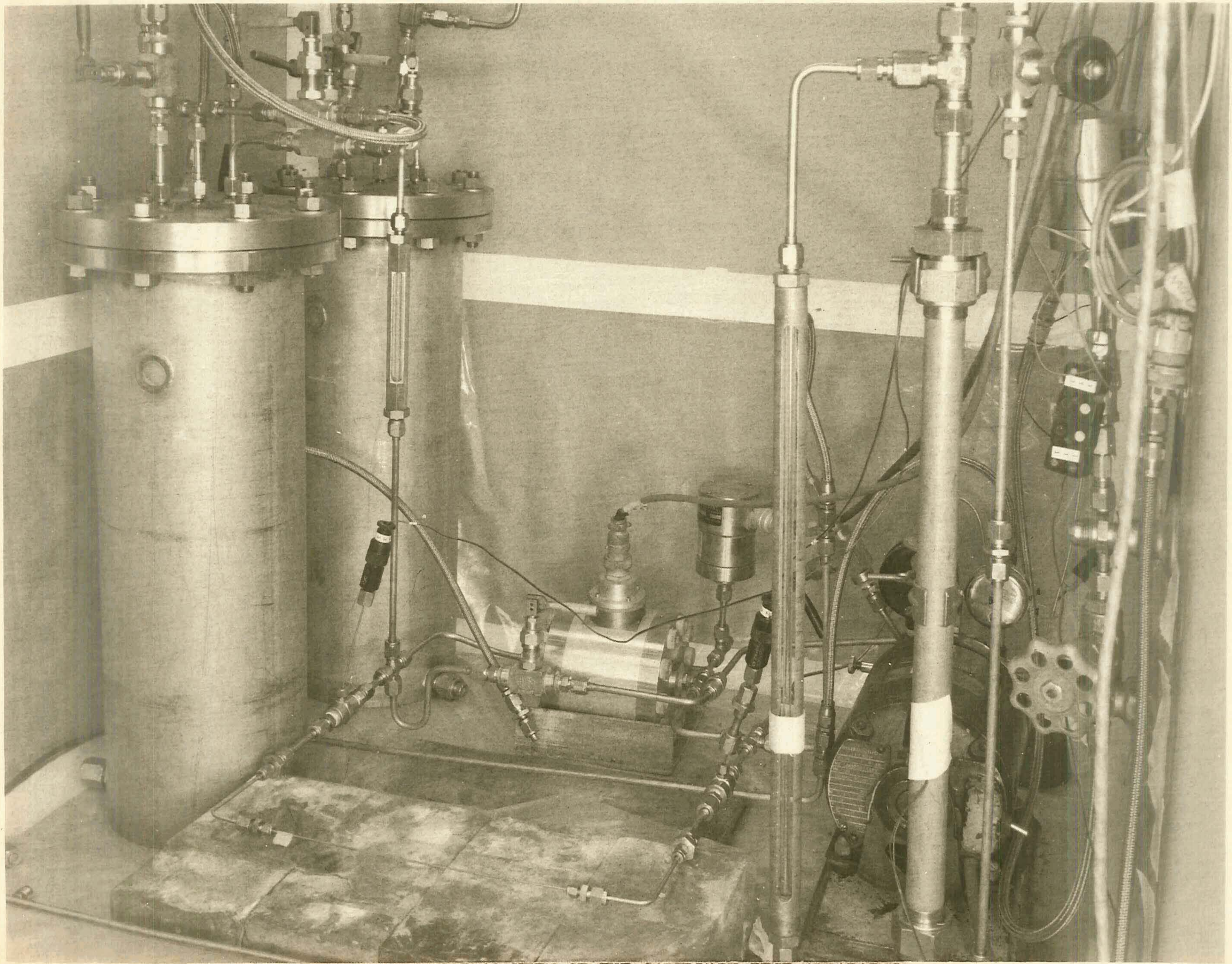

Figure 9: GENERAL VIEW OF THE CAPILLARY TEST APPARATUS

NASA TULALIP - 10M FILTER TEST
SEC. & SETUP - RADIOACTIVE TRACER
TECH. TO DETERMINE FLOW DECAY.
10-5-70

2A295570

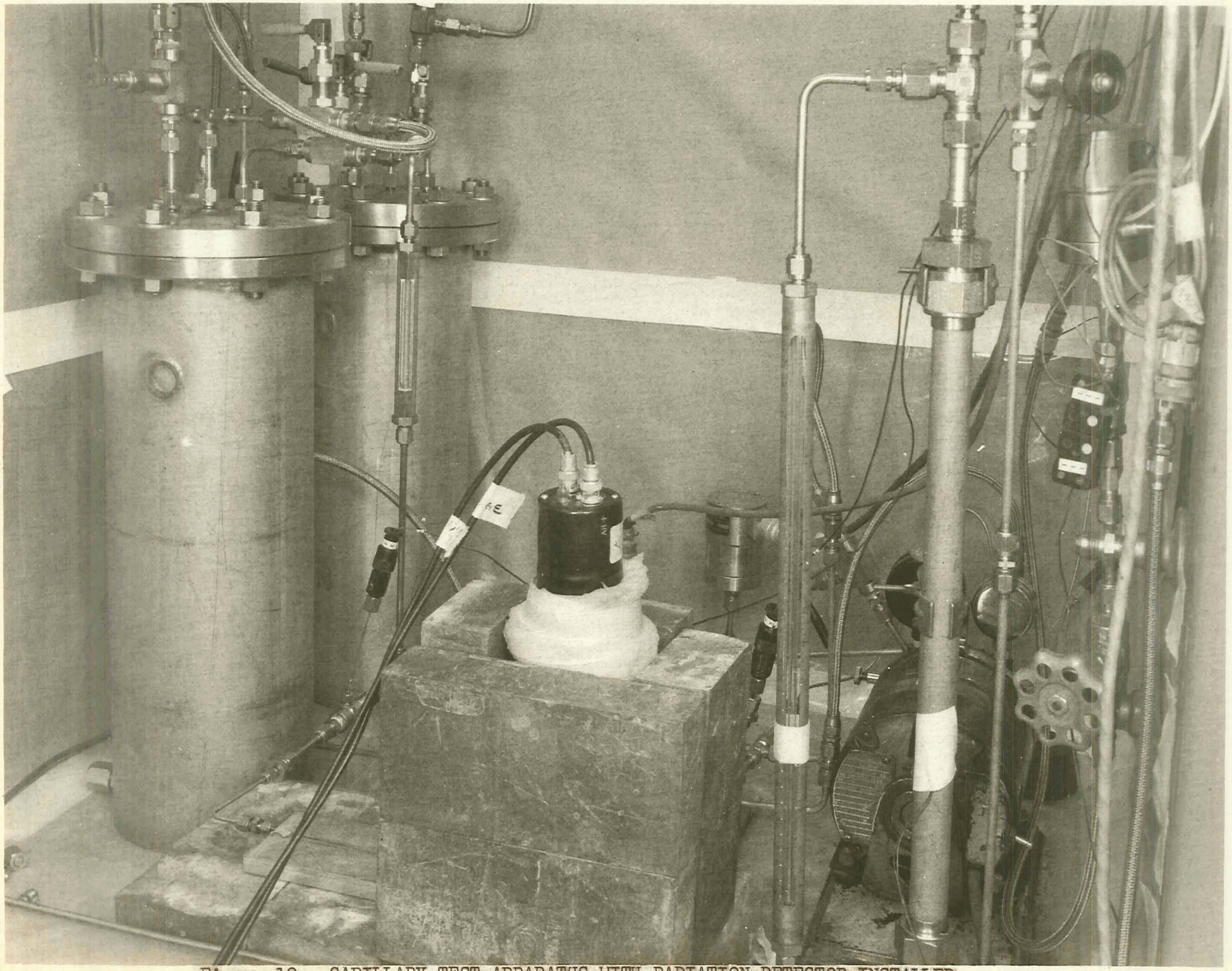

Figure 10: CAPILLARY TEST APPARATUS WITH RADIATION DETECTOR INSTALLED

rinsing, the component was transferred to an acid cleaning solution (Oakite 33). After rinsing, the final immersion was in detergent solution. After the final rinse with deionized water, the component was superficially dried in a stream of nitrogen gas and then placed in an oven for about 2 hours to complete the drying.

In the tests involving filters, a new filter was used in the as-received condition prior to each run. The manufacturer's cleaning procedure consisted of three steps: (1) degreasing with isopropyl alcohol; (2) ultrasonic cleaning in detergent solution, and (3) ultrasonic cleaning in deionized water. The filters were then double sealed in polyethylene bags.

In the case of capillaries, a capillary was cleaned prior to a run. A simple though satisfactory cleaning method consisted of flushing the capillary with deionized water. The capillary was then dried by passing gaseous nitrogen (40 psig) through the capillary, which also served to dislodge any particulate matter which would occasionally remain from a prior run. A water calibration check of the capillary would then yield the proper flow rate, indicating that the capillary was clean.

4.2.2.2 Propellant Handling

In each filter run 2 gallons of propellant was drawn from the main storage tank or drum and placed, in most cases, in the catch tank. The propellant was ready for addition to the feed tank when needed. In some N_2O_4 tests involving distilled propellant, the N_2O_4 was added initially to a third tank. After installing the third tank in the position normally occupied by the catch tank, distillation into the feed tank was accomplished. The distillation occurred rapidly when the bottom of the third tank was warmed to about 100°F and the heat exchanger, through which the N_2O_4 was distilled, was cooled to 32°F.

Since only small quantities of propellant (200 cc) were required for the capillary tests, a 2 gallon tank was filled with the propellant in question prior to the tests from which 200 cc portions were withdrawn as needed. A second 2 gallon tank stored the used 200 cc portions of propellant.

4.2.2.3 Introduction of Radioactive Material into Propellant

In most runs radioactive material was introduced through the manual addition of the desired isotope to the propellant. One millicurie (mc) of each of the three radioisotopes was purchased from International Chemical and Nuclear Corporation (Chemical and Radioisotope Division-Irvine, California). The as-received isotopes were described by the data in Table 5.

TABLE 5. Radioisotope Technical Data as of Reference Date

Item	Fe^{59}	Zn^{65}	Cr^{51}
Chemical Form	Fe(III) in 0.5<u>N</u> HCl	Zn(II) in 0.5<u>N</u> HCl	Cr(III) in 0.5<u>N</u> HCl
Radioactivity Concentration	21.8 mc/ml	33.0 mc/ml	37.4 mc/ml
Volume	0.046 ml	0.03 ml	0.027 ml
Solids Content Concentration	1.55 mg Fe/ml	10 mg Zn/ml	0.205 mg Cr/ml
Solids Content	0.071 mg Fe	0.30 mg Zn	0.0055 mg Cr
Specific Activity	14.0 mc/mg Fe	3.30 mc/mg Zn	178 mc/mg Cr
Radiochemical Purity	99%	99%	99%
Reference Date	4-20-70	4-20-70	4-20-70

Conversion of the metal chloride solutions to metal nitrate solutions (the form of the isotope used for all but the first three runs during this program) was accomplished by diluting the solution to 10 ml with concentrated nitric acid, evaporating the solution down to a volume of about 1 ml at a temperature just less than the boiling point, and diluting back to 10 ml with concentrated nitric acid. From 0.2 ml to 1 ml of solution was used in each run. Prior to the N_2H_4 tests, the concentrated nitric acid solvent was replaced with water in order to prevent ignition of the N_2H_4 by the HNO_3. This was accomplished by evaporating the nitric acid and redissolving the metal nitrate residue in water.

Mixing of isotope with the propellant was achieved by two methods in the filter tests. In the first method the isotope solution was injected with a syringe through a fitting in the top of the feed tank (sometimes before, sometimes after the propellant had been added to the feed tank). The propellant was then vigorously agitated by bubbling nitrogen through the liquid at a high flow rate. The advantage of adding the radioactive solution to the feed tank before flowing in the propellant was that the turbulence caused by the entry of the propellant aided the mixing. However, a disadvantage was that some radioactivity tended to adhere to the bottom surface of the tank which had been contacted by the 0.2 to 1 ml of concentrated radioisotope solution. An improvement was achieved in the second method, which consisted of flowing about 1/3 of the propellant into the feed tank, adding the radioisotope, flowing the remainder of the propellant into the tank, and then bubbling with nitrogen.

In the case of the capillary tests the feed tank was small enough to allow it to be picked up and shaken manually. Consequently, excellent mixing was easily achieved.

In the case of two filter tests the radioactivity was introduced by allowing radioactive foils to interact with the propellant. In the first such test, stainless steel type 304 foil (mass, 9.8 grams; surface area, 300 in^2) was activated for 10 hours in the WSU reactor and was then placed in two gallons of specification grade N_2H_4. The foil had an activity of about 1 mc Cr^{51} and 0.04 mc Fe^{59} at the time of use. The tank containing the foil and propellant was shaken manually twice a day for 10 days. Just prior to the run the radioactive foil was removed from the tank in order to achieve a background reduction. A similar test was conducted with distilled N_2O_4 and radioactive iron foil (mass, 38 grams; surface area, 300 in^2). The iron had an activity of about 0.4 mc and was shaken with the propellant twice a day for 7 days.

4.2.2.4 Propellant Flow

The feed tank in all of the filter runs was initially pressurized at 40 psig. The two gallons of propellant in the feed tank was initially at ambient temperature (close to 70°F). In all of the N_2O_4 runs the propellant was passed through a 32°F heat exchanger prior to entry into the test section. The purpose of the heat exchanger was to increase the chances of flow decay occurring.[2] Most of the N_2H_4 runs did not involve cooling, while in others the heat exchanger bath was held at 43°F. In some of the runs the 2 gallons of propellant was returned to the feed tank for additional passes through the filter. Flow was commenced by opening a throttle valve until the desired flow rate was established (usually 0.2 gal/min.). No more than 30 seconds was required to establish flow.

In the capillary runs flow could be established more quickly, since one did not have to adjust the flow to some predetermined flow rate. Flow was simply set and defined by the desired pressure drop across the capillary (10 or 40 psi). About 200 cc of propellant (initially at about 70°F) was passed through the capillary (sometimes preceded by a heat exchanger) during each run or subrun).

4.2.3 Results and Discussion

Tables 6, 7, 8 and 9 summarize the results of the passage of propellant (to which tracers were added) through filters and capillaries. Table 10 summarizes the results of the metal foil runs. In Tables 6 and 9 the subruns (a), (b), etc. denote recirculation of the 2 gallons of propellant through the filter. In Table 8 the subruns denote a change in the pressure drop across the capillary during a run. The radioactivity added to or present in the propellant is given in gammas per minute, which refers to 0.32 Mev gammas for Cr^{51}, 1.10 Mev gammas for Fe^{59}, and 1.12 Mev gammas for Zn^{65}. Only a small percentage of these gammas are countable (largely because of geometrical limitations). In the case of filters in the metal test section the counting efficiency was 1.12%. In the case of the larger glass test section which forced the detector even farther away from the filter, the efficiency fell to 0.54%. Note that these low counting efficiencies do not jeopardize the sensitivity of the tracer

TABLE 6. N_2O_4 FLOW TESTS (FILTER)

Run	N_2O_4 Condition	Radioactivity Present in N_2O_4 (gammas/minute)	Percent Radioactivity Deposited on Filter	Other Metals Added	Heat Exchanger Temperature	ΔP Across Filter, psi, (initial)	(final)	Initial Flow Rate, gal/min	Percent Flow Decay
1	MSC-PPD-2A	1.92×10^8 Fe^{59}	4.35	None	32°F	1	35	0.2	100
2	Distilled	1.87×10^8 Fe^{59}	4.44	None	"	1.8	1.8	0.2	0
3	"	1.79×10^8 Fe^{59}	0.64	0.1 ppm Fe	"	1.8	1.8	0.2	0
4	"	1.76×10^8 Fe^{59}	0.42	1.0 ppm Fe	"	2.5	27	*	77*
5	"	1.76×10^8 Fe^{59}	0.88	0.3 ppm Fe	"	1	3	0.2	15
6(a)	MSC-PPD-2A	7.09×10^6 Cr^{51}	19.9	None	"	2	7	0.22	0
(b)	"	6.58×10^6 Cr^{51}	11.1	"	"	7	31	0.23	62
(c)	"	6.61×10^6 Cr^{51}	3.63	"	"	2	19	0.2	100
7(a)	"	1.07×10^7 Fe^{59} + Zn^{65} + Cr^{51}	3.07	"	"	2	19	0.2	25
(b)	"	1.03×10^7 Fe^{59} + Zn^{65} + Cr^{51}	2.69	"	"	18	32	0.2	100
8(a)	"	1.57×10^8 Zn^{65}	3.01	"	"	2	10	0.2	15
(b)	"	1.52×10^8 Zn^{65}	0.33	"	"	15	22	0.18	31
9(a)	"	1.55×10^8 Zn^{65}	4.85	"	"	2	2	0.2	0
(b)	"	1.47×10^8 Zn^{65}	2.64	"	"	2	2	0.2	0
(c)	"	1.43×10^8 Zn^{65}	1.19	"	"	2	2	0.2	0
(d)	"	1.41×10^8 Zn^{65}	0.51	"	"	2	2	0.2	0

* Flow meter failed before the flow rate was established. Percent flow decay was estimated from the pressure drop across the filter.

TABLE 6. N_2O_4 FLOW TESTS (FILTER) (cont.)

Run	N_2O_4 Condition	Radioactivity Present in N_2O_4 (gammas/minute)	Percent Radioactivity Deposited on Filter	Other Metals Added	Heat Exchanger Temperature	ΔP Across Filter, psi, (initial)	(final)	Initial Flow Rate, gal/min	Percent Flow Decay
9(e)	MSC-PPD-2A	1.41×10^8 Zn^{65}	-0.19	None	32°F	2	2	0.2	0
(f)	"	"	0.25	"	"	"	"	"	"
(g)	"	"	0.32	"	"	"	"	"	"
(h)	"	"	0.38	"	"	3	5	0.38	5
(i)	"	1.40×10^8 Zn^{65}	0.32	"	"	3.5	7.5	0.36	7
(j)	"	"	0.44	"	"	1.3	6.5	0.2	15
10(a)	Distilled	1.55×10^8 Zn^{65}	2.39	"	"	2	2	0.2	0
(b)	"	1.51×10^8 Zn^{65}	1.69	"	"	1.5	1.5	0.2	0
(c)	"	1.49×10^8 Zn^{65}	1.74	"	"	1	1	0.2	0
(d)	"	1.46×10^8 Zn^{65}	1.26	"	"	1	1	0.2	0
(e)	"	1.44×10^8 Zn^{65}	0.16	"	"	2	2	0.2	0
(f)	"	"	0.37	"	"	2	4	0.21	2
(g)	"	1.43×10^8 Zn^{65}	0.27	"	"	2	5.8	0.21	14
(h)	"	"	0.19	"	"	1	6	0.21	10
(i)	"	"	0.19	"	"	1.5	7.5	0.21	14
(j)	"	1.42×10^8 Zn^{65}	0.12	"	"	6	11.5	0.36	7
(k)	"	"	0.27	"	"	10	14.5	0.33	7
(l)	"	"	0.20	"	"	10.5	16	0.32	10
(m)	"	"	0.14	"	"	12	17.6	0.31	13
(n)	"	"	0.18	"	"	13	17.7	0.31	9

TABLE 7. N_2O_4 FLOW TESTS (CAPILLARY)

Run	Condition	Radioactivity Present in N_2O_4 (gammas/Minute)	Percent Radioactivity Deposited in Capillary	Capillary	Heat Exchanger Temperature	ΔP Across Capillary, psi	Flow Rate, ml/min			
							(Initial)	(Max)	(Min)	(Final)
11	MSC-PPD-2A	None	-	#2-8 mil	70°F	40	3.6	4.5	3.5	4.3
12	"	"	-	#1-8 mil	Variable(70-32°F)	40	2.8	5.5	2.8	5.5
13	"	"	-	#1-8 mil	Variable(70-32°F)	10	2.7	2.7	1.7	1.7
14	"	4.32×10^7 $Fe^{59} + Zn^{65} + Cr^{51}$	0	#1-8 mil	32°F	10	2.6	2.6	1.8	2.3

TABLE 8. N_2H_4 FLOW TESTS (CAPILLARY)

Run	Condition	Radioactivity Present in N_2H_4 (gammas/Minute)	Percent Radioactivity Deposited in Capillary	Capillary	Heat Exchanger Temperature	ΔP Across Capillary, psi	Flow Rate, ml/min			
							(Initial)	(Max)	(Min)	(Final)
15	MIL-P-26536C	"	-	#3-13 mil	43°F	10	7.1	11.1	5.6	11.1
16(a)	"	"	-	#1-8 mil	43°F	40	3.6	3.8	3.4	3.4
(b)	"	"	-	"	"	10	0.96	0.97	0.76	0.90
(c)	"	"	-	"	"	40	3.2	3.2	3.1	3.1
17(a)	"	"	-	#2-8 mil	"	10	1.1	1.1	0.54	0.54
(b)	"	"	-	"	"	40	2.3	2.7	2.3	2.6
18(a)	"	3.70×10^7 Zn^{65}	0	"	"	40	1.9	1.9	1.8	1.8
(b)	"	"	0	"	"	10	0	0	0	0
19(a)	"	None	-	"	70°F	40	3.7	3.7	3.5	3.6
(b)	"	"	-	"	"	10	0.89	0.92	0.89	0.92
20	"	"	-	"	"	10	1.0	1.0	0.03	0.67
21	"	"	-	"	"	10	0.85	0.91	0.78	0.81

TABLE 9. N_2H_4 FLOW TESTS (FILTER)

Run	N_2H_4 Condition	Radioactivity Present in N_2O_4 (gammas/minute)	Percent Radioactivity Deposited on Filter	Other Metal Added	Heat Exchanger Temperature	ΔP Across Filter, psi (initial)	ΔP Across Filter, psi (final)	Initial Flow Rate, gal/min	Percent Flow Decay
22	MIL-P-26536C	None	-	None	70°F	3	3	0.2	0
23(a)	"	1.96×10^7 Fe^{59}	0.50	"	"	"	"	"	"
(b)	"	1.95×10^7 Fe^{59}	0.36	"	"	"	"	"	"
(c)	"	"	0.09	"	"	"	"	"	"
(d)	"	1.94×10^7 Fe^{59}	0.23	"	"	"	"	"	"
24(a)	"	9.36×10^7 Fe^{59} + Zn^{65}	0.30	"	"	"	"	"	"
(b)	"	9.33×10^7 Fe^{59} + Zn^{65}	0.15	"	"	"	"	"	"
25(a)	"	9.49×10^7 Fe^{59} + Zn^{65} + Cr^{51}	0.10	"	"	"	"	"	"
(b)	"	9.48×10^7 Fe^{59} + Zn^{65} + Cr^{51}	0.11	"	"	"	"	"	"
(c)	"	9.47×10^7 Fe^{59} + Zn^{65} + Cr^{51}	0.14	"	43°F	"	"	"	"
(d)	"	9.46×10^7 Fe^{59} + Zn^{65} + Cr^{51}	0.07	"	"	"	"	"	"
(e)	"	"	0	"	"	"	"	"	"
(f)	"	9.45×10^7 Fe^{59} + Zn^{65} + Cr^{51}	0.09	"	"	"	"	"	"
(g)	"	"	0	"	"	12	12	0.38	"

TABLE 9. N_2H_4 FLOW TESTS (FILTER) (continued)

Run	N_2H_4 Condition	Radioactivity Present in N_2O_4 (gammas/minute)	Percent Radioactivity Deposited on Filter	Other Metal Added	Heat Exchanger Temperature	ΔP Across Filter, psi (initial)	ΔP Across Filter, psi (final)	Initial Flow Rate, gal/min	Percent Flow Decay
26(a)	"	8.20×10^8 Fe^{59} + Zn^{65} + Cr^{51}	0.31	None	70°F	*	*	0.2	0
26(b)	MIL-P-26536C	8.18×10^8 Fe^{59} + Zn^{65} + Cr^{51}	0.09	"	70°F	*	*	0.2	"
(c)	"	8.17×10^8 Fe^{59} + Zn^{65} + Cr^{51}	0.08	"	"	*	*	"	"
27	"	8.16×10^8 Fe^{59} + Zn^{65} + Cr^{51}	-0.29	28 ppm Zn	"	12	21	0.21	24

* Instrumentation Failure

TABLE 10. ACTIVATED FOIL DISSOLUTION TESTS

Run	Propellant	Propellant Condition	Radioactive Foil	Dissolved Metal Content From Foil	Percent of Dissolved Metal Deposited on Filter	Heat Exchanger Temperature	ΔP Across Filter, psi (initial)	ΔP Across Filter, psi (final)	Initial Flow Rate, gal/min	Percent Flow Decay
28	N_2H_4	MIL-P-26536C	304 Stainless Steel	0.6 ppm Fe 0.01 ppm Cr	Not Determined	70°F	*	*	0.2	*
29	N_2O_4	Distilled	Iron	0.2 ppm Fe	12.4% Fe**	32°F	7.5	38	0.2	100

* Blockage of filter occurred, traced to extraneous particulate matter

** In six passes of two gallons of N_2O_4 through the filter technique. Gamma emission rates of the order of 10^8 gammas per minute are encountered in Tables 6, 7, 8, and 9. Although only about 1% of these emissions are countable, the resulting count rate of 10^6 cpm is still very high.

Generally speaking, flow decay was readily observed when MSC-PPD-2A N_2O_4 was passed through the 10 micron absolute filters, but no flow decay was found when similar tests were conducted with freshly distilled N_2O_4. Deposition of significant amounts of radioactivity was detected in all of the N_2O_4/filter tests, sometimes prior to the point at which a decrease in flow rate could be measured. Figures 11 and 12 illustrate certain results that are in many ways typical of all of the N_2O_4/filter tests.

Figure 11 (run 1) shows flow decay setting in immediately at the start of the run, accompanied by an increase in the pressure drop across the filter and a build-up of radioactivity on the filter. Over 50% flow decay had occurred after just 6 minutes time. The high sensitivity of the tracer technique can be appreciated when one considers that the high count rate in Figure 11 ($\sim$ 30,000 cpm) was obtained through the addition of only 0.001 ppm of tracer iron to the N_2O_4, and only 4.35% of this amount (Table 6) deposited on the filter.

In some runs the N_2O_4 had to be recirculated through the filter before appreciable flow decay could be detected. Figure 12 shows that in run 8 (a) flow decay started after about 2 minutes (although Zn^{65} radioactivity build-up started at once), but only about 15% flow decay had occurred at the conclusion of this run. A second pass of this same two gallons of N_2O_4 through the filter (run 8(b)) produced considerably more flow decay, but the build-up of Zn^{65} tracer continued at a much slower rate. In all runs where the N_2O_4 was recirculated, the first pass through the filter deposited the greatest amount of radioactivity, suggesting that some sort of equilibrium or steady state condition is quickly reached.

In general, flow decay was not observed when N_2H_4 was passed through filters. Furthermore, relatively little radioactive material deposited on the filters,

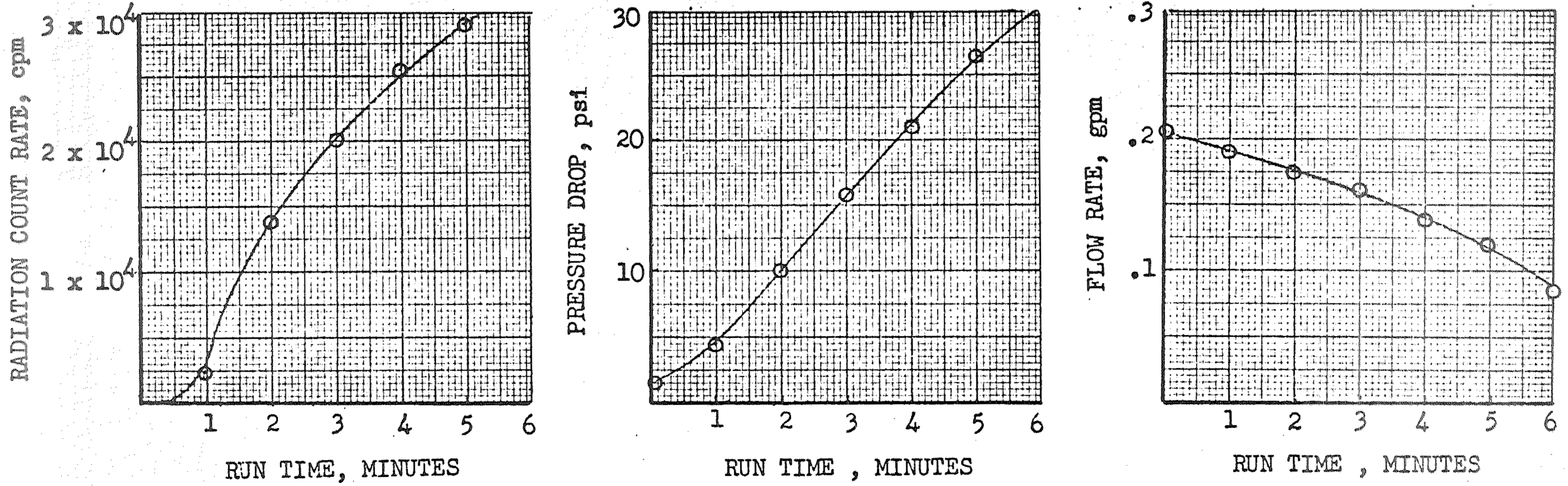

Figure 11: TIME HISTORY OF TEST PARAMETERS DURING RUN 1

(Propellant - N_2O_4, Tracer - Fe^{59}, Filter)

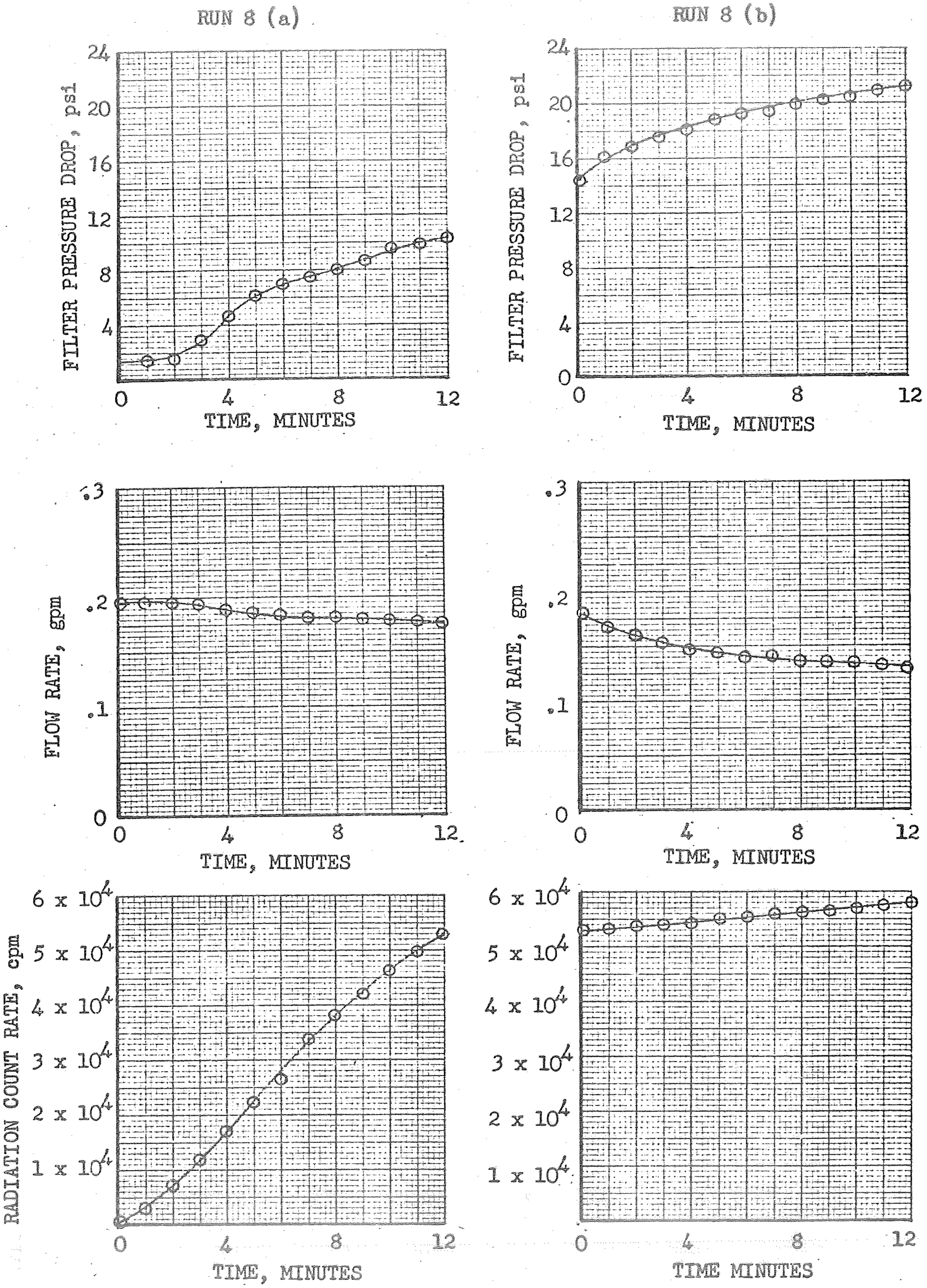

Figure 12: TIME HISTORY OF TEST PARAMETERS DURING RUN 8 (Propellant - N_2O_4, Tracer - Zn^{65}, Filter)

being typically only about 5 to 10% of the amount that deposited in the case of the N_2O_4 tests. Figure 13 records the typical level flow rate, level pressure drop, and small increase in Fe^{59} radiation count rate. The count rate was plotted on a scale similar to those of Figures 11 and 12 so that a comparison of the relative radiation build-up for the N_2O_4 and N_2H_4 tests could be viewed in the proper perspective.

Capillary tests for N_2O_4 and N_2H_4 were similar in that no build-up of radioactivity could be detected in the capillaries. Although some flow irregularities were observed, the evidence was suggestive of clogging by extraneous particulate matter rather than by a classical flow decay mechanism such as complex formation or gelation. Figure 14 is a typical example (run 14) showing no count rate increase and minor flow irregularities.

4.2.3.1 N_2O_4 Filter Tests

Prior to run 1, a checkout run was made. Both the flow meter and radiation detector failed to operate, but the final ΔP across the filter (~ 35 psi) indicated that flow decay had occurred strongly.

In run 1 flow decay also occurred strongly, with essentially complete blockage of the filter reached after about 8 minutes. The increase in the ΔP across the filter paralleled the decrease in flow rate. The tracer used in run 1 was a 1 ml aqueous solution of $Fe^{59}Cl_3$ (1/10 of the solids content of Fe^{59} in Table 5). From Table 5 one can see that this is only 7.1×10^{-6} grams of iron. Since the two gallons of N_2O_4 weighs approximately 10^4 grams, the tracer content corresponded to only 0.0007 ppm iron, an amount so small that no perturbation of the iron content already present in the MSC-PPD-2A N_2O_4 would be expected. Nor would the water content be likely to disturb the system, 1 ml of water accounting for only 0.01%, far under the spec limit of 0.1%. Of considerable interest was the fact that only 4.35% of the $FeCl_3$ tracer added was deposited on the filter. Assuming that the $Fe^{59}Cl_3$ equilibrates with the iron compounds already present in solution (about 0.7 ppm from Table 3) through intermolecular exchange of iron atoms or some such mechanism (e.g., $Fe^{59}Cl_3 + Fe(NO_3)_3 \cdot N_2O_4 = FeCl_3 + Fe^{59}(NO_3)_3 \cdot N_2O_4$) and assuming that the iron

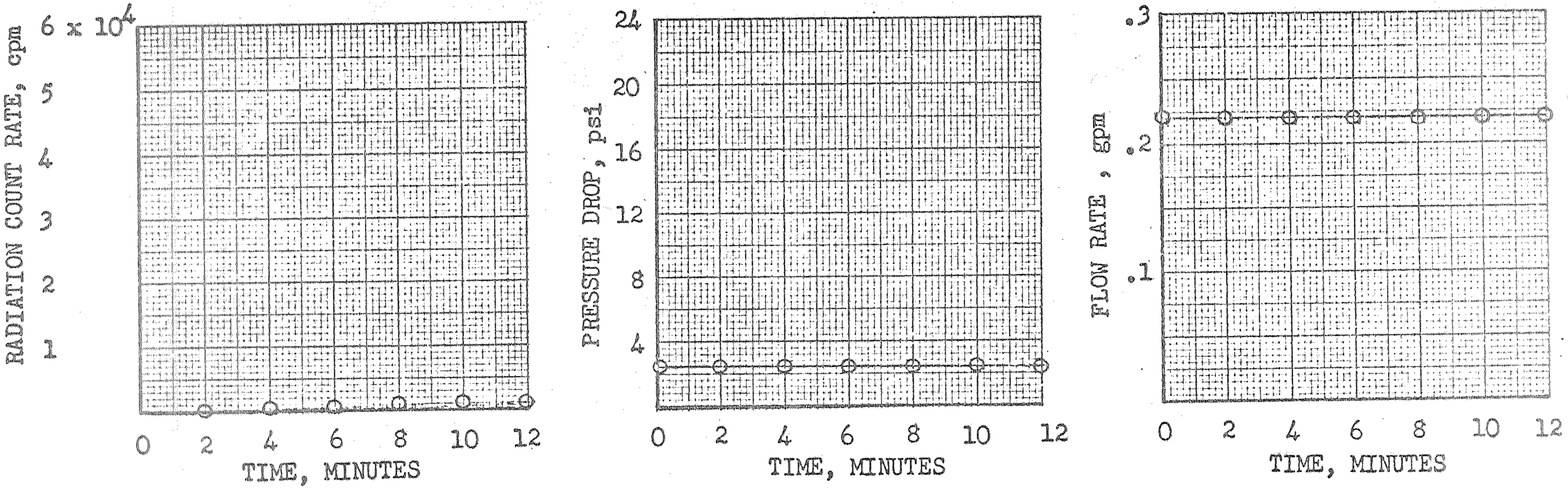

Figure 13: TIME HISTORY OF TEST PARAMETERS DURING RUN 23 (a)
(Propellant - N_2H_4, Tracer- Fe^{59}, Filter)

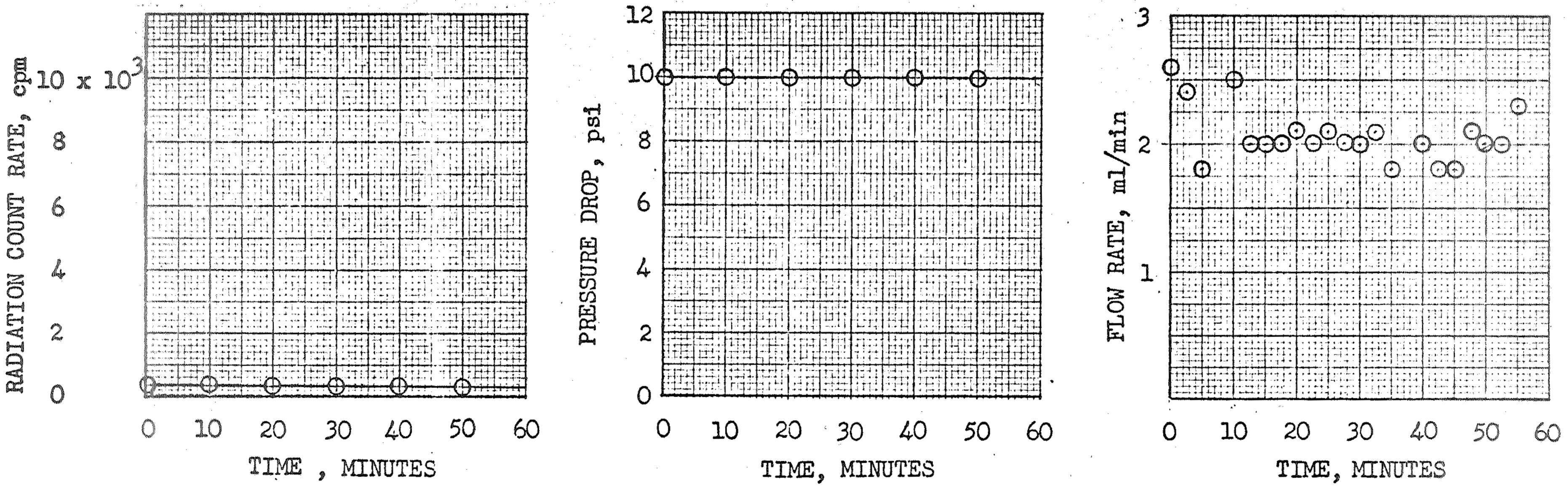

Figure 14: TIME HISTORY OF TEST PARAMETERS DURING RUN 14

(Propellant- N_2O_4, Tracers- Cr^{51}, Fe^{59}, Zn^{65}, Capillary) compounds are responsible for flow decay, then only a small portion of the already small 0.7 ppm iron content actually is responsible for the clogging.

Run 2 was performed with distilled N_2O_4. Since distillation is known to produce iron-free N_2O_4,[1,3] it was thought that distillation might be a means of eliminating flow decay, provided that the rate of reaction of the N_2O_4 with the stainless steel tank walls did not regenerate the iron compounds at a fast rate. This was apparently the case, because no flow decay was observed in run 2. Of interest is the fact that about the same amount of radioactivity (4.44% of the Fe^{59} added) deposited on the filter as in run 1. This is not, however, the same amount of iron, provided that the intermolecular exchange mechanism mentioned above is operable. Assuming that in run 1 the Fe^{59} underwent exchange with the 0.7 ppm Fe already present in the N_2O_4 (Table 3), then this would mean about 1000 times more iron deposited on the filter in run 1 than in run 2 (in which only 0.0007 ppm of tracer iron was present).

Run 2 suggested a need for determining percent flow decay as a function of iron concentration. Consequently, in the next three runs varying amounts of iron as $Fe(NO_3)_3$ were added: run 3, 0.1 ppm; run 4, 1.0 ppm; run 5, 0.3 ppm. The $Fe(NO_3)_3$ was prepared by dissolving the desired weight of iron wire in concentrated nitric acid. The N_2O_4 used in run 3 was the same two gallons of N_2O_4 left from run 2. A new filter was installed, and the $Fe^{59}Cl_3$ left from run 2 remained in the propellant. Run 4 (and other Fe^{59} runs thereafter) marked the beginning of the use of $Fe^{59}(NO_3)_3$ dissolved in 0.2 to 1 ml concentrated HNO_3 as the tracer. Interestingly enough, the flow meter recorded no flow decay with 0.1 ppm Fe, 15% flow decay with 0.3 ppm, and 77% flow decay with 1.0 ppm. Thus the degree of flow decay seemed directly related to the amount of $Fe(NO_3)_3$ added. In the 1.0 ppm run, the flow meter failed before the equilibrium flow rate was established, and the percent flow decay was estimated from the change in the pressure drop across the filter. In all three runs the deposition of Fe^{59} was observed. The percent Fe^{59} that deposited (run 3, 0.64%; run 4, 0.42%; run 5, 0.88%) was, however, about an order of magnitude less than in run 2. This is probably at least in part due to the 0.1-1 ppm Fe as $Fe(NO_3)_3$ added in runs 3-5, which had the effect of diluting the specific activity of the Fe^{59}.

Some difficulty was encountered in achieving uniform mixing of the $Fe(NO_3)_3$ in the N_2O_4 in runs 4 and 5. Dispersing uniformly a very small amount of a solution in a large volume is notoriously difficult, but the problem in this case was compounded by the apparent settling of the $Fe^{59}(NO_3)_3$ upon addition of the 1 ml of $Fe^{59}(NO_3)_3/HNO_3$ solution to the N_2O_4. Settling was monitored by placing the NaI scintillation detector at various points along the outside of the feed tank. In run 4 after adding the $Fe(NO_3)_3$ solution through a fitting in the top of the tank, it was found that about 2/3 of the $Fe(NO_3)_3$ was located in the bottom half of the tank after only 2 minutes. The N_2O_4 was then vigorously agitated by bubbling nitrogen through the liquid at a high flow rate. This procedure improved the distribution of the $Fe(NO_3)_3$, but some still tended to settle towards the bottom.

Three explanations are available for the settling. First, 100% HNO_3 is largely insoluble in N_2O_4 and the higher density of the HNO_3 (HNO_3,1.50 g/ml; N_2O_4, 1.44 g/ml) results in settling upon addition to N_2O_4. The concentrated (70%) HNO_3 is rapidly converted to 100% HNO_3 through the reaction of the water in the HNO_3 solution with N_2O_4. The denser HNO_3 containing the dissolved Fe^{59} would then settle and carry the radioactivity to the bottom of the tank. It should be noted, however, that in this case the iron would be in true solution, even though the solvent would be small globules of 100% HNO_3. The second possibility is that $Fe(NO_3)_3$ is precipitated upon contact of the $Fe(NO_3)_3/HNO_3$solution with N_2O_4. $Fe(NO_3)_3$ is apparently soluble to the extent of about 1 ppm in N_2O_4 at room temperature [1,3]; so,the two gallons of N_2O_4 can certainly accommodate in true solution the amount of $Fe(NO_3)_3$ added in runs 4 and 5. However, precipitation may occur due to localized supersaturation when the $Fe(NO_3)_3$ solution contacts the N_2O_4. The precipitate would redissolve given enough time, but an appreciable length of time might be required. The third explanation is that iron compounds tend to exist in N_2O_4 in a colloidal state[2,4] and that some settling of the colloid occurs. It is interesting that in run 6 the Cr^{51} tracer also tended to settle, but in runs 8, 9, and 10, in which Zn^{65} was added, perfectly uniform distribution was quickly and easily achieved. It is possible that zinc nitrate is more soluble in N_2O_4 than iron or chromium nitrate. It may be noteworthy that no settling of any of the three isotopes was detected in hydrazine (Sections 4.2.3.4 and 4.2.3.5). The solubilities of metal salts are reported to be relatively high in hydrazine.[4]

In run 6 the glass test section was replaced with a stainless steel test section (compare Figures 6 and 7). The purpose of the glass housing had been to permit visual observation of any deposition that might occur on the filter. No deposits were observed with the unaided eye. The deposits could probably have been readily seen with the careful use of a microscope, but this matter was not pursued further because flow decay deposits on this type filter have been visually observed previously and the deposition process documented on film.[2]

In run 6(a) no flow decay was observed, although radioactive material deposited on the filter and just before the conclusion of the run a slight increase in the ΔP across the filter was noted, which were regarded as signs that flow decay would probably start early in run 6(b). This was found to be the case with 62% flow decay occurring during the second pass of the propellant through the filter.

Chromium-51 was added as the tracer in run 6. Runs 6(a) and 6(b) were notable for the large percentages of the tracer that deposited (20 and 11%). Run 6(b) was the first of several runs in which some of the deposit was lost at the conclusion of the run. This occurred at shutdown when a small back-surge of propellant dislodged some of the deposit as indicated by the decrease in radioactivity. Although 19.9% of the radioactivity had deposited in run 6(a), the backsurge removed about 64% of this. That is why the radioactivity listed as being present in the N_2O_4 in run 6(b) is not 19.9% less than the starting amount in run 6(a). The results of the backsurge suggested that perhaps all of the deposit could be removed by flowing the N_2O_4 back through the filter in the reverse direction. This was attempted at the conclusion of run 6(b).

About 60% of the radioactivity was eliminated by this procedure, but the remaining material adhered tenaciously to the filter and could not be removed. Run 6(c) produced 100% flow decay adding 3.6% more Cr^{51} to the filter, which after allowing for the losses due to the backsurges corresponded to less radioactive deposit on the filter than at the end of run 6(a).

In runs 7 and 8 flow decay began in 7(a) and 8(a), but an additional pass through the filter was required to establish substantial flow decay or complete blockage. In run 7 the count rate was measured in the 1.1 Mev energy region. The tracer mixture was derived from 0.25 ml Cr^{51}, 0.01 ml Zn^{65}, and 0.02 ml Fe^{59} solutions.

Run 9 was very interesting in that after seven consecutive passes through the filter, no sign of a flow rate decrease had occurred. Radioactive Zn^{65} deposition increased only very slowly after run 9(d), to which point about 9% of the available $Zn^{65}(NO_3)_3$ had deposited. Since no flow decay seemed imminent, a decision was made to double the flow rate on the eighth pass, 9(h). The reasoning was that the increased flow rate might dislodge any material that had deposited on the filter. Upon doubling the flow rate, flow decay began almost immediately, and the flow rate decreased about 5% in run 9(h). Another pass was made, and the flow rate decreased another 7%, for a total decrease of 12%. To check whether flow decay would continue if the flow rate were reduced back to the original value (0.2 gal/min), run 9(j) was tried. Flow decay did indeed continue, with a 15% decrease in run 9(j). It is certainly possible to deposit small ($< 10\,\mu$) particles on a wire mesh type filter without partially blocking the holes, since small particles of a contaminant metal complex can attach to the front or back of the wires primarily parallel to the direction of flow.

As previously noted (Section 4.1.2.2) the iron (and other metals) concentration in the main N_2O_4 storage tank may be greater at the bottom of the tank. This would increase the chances of flow decay occurring in the early runs, because the siphon tube, which extends close to the bottom of the storage tank, would withdraw N_2O_4 that was richer in particulate iron than the last portions of N_2O_4 removed. Although more data are required for proof, the data of Table 6 are nevertheless consistent with the hypothesis that flow decay should occur most readily in the early runs. In only a single run (run 1) was complete blockage noted for the first pass of MSC-PPD-2A N_2O_4 through the filter. In subsequent runs (6, 7 and 8) two or three passes through the filter were needed to cause complete or substantial blockage. (Runs 2, 3, 4, and 5 were made with distilled N_2O_4 and are therefore not applicable.) The final run with spec grade propellant (run 9) was made after about 80 to 90% of the N_2O_4 in the storage tank had been used. As noted above, in this run flow decay occurred with only great difficulty.

Run 10 was another test with distilled N_2O_4. The purpose was to see if flow decay would occur with distilled N_2O_4 that had been recirculated through the filter as in runs 6-9. Zinc-65 was added as the tracer. No flow decay was observed in the first four passes, although Zn^{65} deposited on the filter as usual(in run 10(a), 2.39% of the added Zn^{65} deposited with diminishing amounts in runs (b)-(d)). At this point the testing was ended for the day and the N_2O_4 was allowed to stand overnight in the feed tank. The next morning about 16 hours later the testing was resumed. In 10(e) no flow decay occurred, but in the very next pass through the filter (10(f)) flow decay began and continued for the remainder of run 10. These results probably indicate that the rate of reaction of the N_2O_4 with the walls of the stainless steel tank is fast enough to regenerate a substantial amount of dissolved iron (or other metal compounds) within a period of a few hours. The surface area to propellant volume ratio of the tank is fairly large and the dissolution rate would accordingly be high. That the N_2O_4 would be nearly saturated with iron upon standing for about one day would be consistent with various published rate data[1,3], although effects on the rate such as the presence or absence of stirring are not known with certainty.

Table 10 lists the activated foil dissolution tests. Radioactive iron foil (rather than stainless steel) was selected for run 29 in part because its rate of dissolution had been previously determined.[3] Calculations before the run indicated that a week's contact between the propellant and the radioactive iron foil would be sufficient to approach saturation. The effect of the stainless steel surface of the feed tank was an unknown factor, but because the two surface areas were comparable (each approximately 300 in^2), one would expect to obtain substantial Fe^{59} activity within the propellant even if the rate of dissolution of the stainless steel were somewhat faster. This was found to be the case. The iron concentration from the iron foils was determined to be about 0.2 ppm. The total iron concentration was no doubt higher on account of the contribution from the tank walls. On the fourth pass through the filter flow decay began and continued for two more passes through the filter. Near the beginning of the sixth pass complete blockage occurred. At the conclusion of the sixth pass, Fe^{59} on the filter and in an aliquot of N_2O_4 were counted in the NaI well detector used in Task 1 so that the ratio of iron on the filter to that remaining in the propellant could be accurately established. This measurement also permitted determination of the amount of iron that had dissolved from the radioactive iron foil. The gamma count rate on the filter (790 cpm) was found to be 12.4% of the original total count rate in the N_2O_4. This degree of deposition is in reasonably good agreement with the results of Table 6, confirming that only a small percentage of the iron in solution deposits on the filter during or preceding the flow decay process and suggesting that manual tracer addition is a valid way of introducing radioactivity into the propellant.

Interesting results were obtained when attempts were made to clean the filters. All filters which had been subsequently exposed to the air did not exhibit any visible contamination, even though considerable radioactive material had deposited on the filter. These filters were rinsed with various solvents and monitored during the rinsing process for removal of radioactivity. The filter from run 4 was typical. It was rinsed with (in order) water, acetone, ammonium hydroxide, and potassium cyanide solution. None of these solvents had any apparent effect; all of the radioactivity remained with the filter. The next rinsing was with nitric acid (diluted 1 to 4 by volume), which removed all of the radioactivity very quickly and efficiently. More data are necessary before the reason for the effectiveness of nitric acid as a cleaning agent can be explained.

4.2.3.2 Capillary Tube Calibrations

Prior to the tests the two 8-mil capillaries were calibrated with water. Since the Reynolds numbers encountered in this program were less than 2000, laminar flow was expected in all of the runs. For laminar flow the volumetric flow rate is directly proportional to the pressure drop across the capillary and the fourth power of the diameter and inversely proportional to the length of the capillary and the viscosity of the fluid. For a given capillary the volumetric flow rate is simply inversely proportional to the viscosity at a fixed pressure drop. Table 11 summarizes the flow rates found for H_2O and lists the calculated values for N_2O_4 and N_2H_4 based on the viscosity ratios.

TABLE 11. CAPILLARY FLOW RATES AT 67°F

Capillary Tube Number	ΔP (psi)	H_2O Flow Rate Found (ml/min)	N_2O_4 Flow Rate Calculated (ml/min)	N_2H_4 Flow Rate Calculated (ml/min)
1	10	1.01	2.59	1.10
1	40	3.91	10.03	4.27
2	10	0.89	2.27	0.97
2	40	3.42	8.77	3.74

The first conclusion of Table 11 is that the flow rate of capillary number 1 is about 14% greater than that of capillary number 2. The second conclusion is that the flow rate as expected is very nearly directly proportional to the ΔP across the filter, although the flow rate did not quite quadruple when the ΔP was quadrupled.

4.2.3.3 N_2O_4 Capillary Tests

The flow rates listed in Table 7 did not in general agree completely with the theoretical flow rates given in Table 11. Also irregularities in flow are apparent, although no trend of a decrease in flow rate with time can be seen. Runs 13 and 14 showed good agreement with the theoretical flow rate (Table 11) at the start of the run, but the flow rates then decreased later in the runs (to 1.7 and 1.8 ml/min, respectively). In run 14 the flow rate increased towards the end of the run and again approached the theoretical flow rate. The flow irregularities seem more consistent with partial clogging from extraneous particulate matter rather than from flow decay mechanisms such as gelation or complex formation. For example, in run 12 flow did not start when the propellant in the capillary was first pressurized to 40 psi. After recleaning, flow began at a low flow rate (2.8 ml/min) and then began to increase midway through the run, finishing at 5.5 ml/min, nearly double the starting flow rate. The fact that flow would not start initially and that when it finally did start the flow rate actually increased with time is more consistent with simple particulate matter clogging than a flow decay mechanism. Furthermore, in run 14 no radioactivity could be detected as having deposited in the capillary. In some of the runs the propellant was cooled prior to entry into the test section, but the flow rates were so small that the propellant had warmed back to 70°F before entry into the capillary, meaning that viscosity variations with temperature cannot account for the flow irregularities of Table 7.

The flow rates of Table 7 are probably accurate to ±5% at best. The graduated sight gauge markings were only 5 ml apart, which permitted many flow rate readings to be made, but limited the accuracy in any one individual reading.

4.2.3.4 N_2H_4 Capillary Tests

Like the N_2O_4 flow runs the N_2H_4 tests also exhibited some flow rate irregularities, but in this case the flow rates seemed in better agreement with theoretical values. Again no flow decay trend could be discerned, and the flow irregularities are best explained by partial clogging due to extraneous particulate matter. No deposition of radioactive matter was detected.

Runs 16(a) and (b), 19, and 21 yielded flow rates that were fairly close to theoretical (Table 11). Also the initial flow rates in runs 17(a) and 20 were in good agreement with theory. In run 16 the first portion of the run, 16(a), was conducted at 40 psi. In the midst of the run the head pressure was suddenly reduced to 10 psi to see if the flow rate would be reduced by a factor of 4. Such was found to be the case, with the flow rate dropping from about 3.6 ml/min to about 0.9 ml/min. However, when the head pressure was returned to 40 psi in 16(c), the flow rate increased to 3.2 ml/min, not quite equal to the original value in run 16(a). Runs 19(a) and (b) were in excellent agreement with theory and run 21 was satisfactory as well.

Runs 18(b) and 20 were the only runs in which substantial (complete or almost complete) blockage occurred. Flow would not even begin in run 18(b) when the pressure was reduced a factor of 4 from 18(a). In run 20 flow began well, but then decreased to almost nothing. It was thought that if a particle were blocking the capillary a sharp tap might dislodge the particle. Upon sharply tapping the capillary with a wrench the flow rate suddenly increased from 0.3 ml/min to 0.67 ml/min. At the conclusion of this run an examination of the capillary revealed black specs at the entrance to the capillary. These black specs, which apparently had been responsible for clogging the capillary, had more the appearance of extraneous particulate matter (such as described in Section 4.2.3.5 and Figure 15) rather than a metal complex compound.

4.2.3.5 N_2H_4 Filter Tests

The N_2H_4 flow tests of Table 9 (runs 22-26) were very satisfying in that not only no flow decay occurred, but the amount of radioactivity that deposited on the filter was about an order of magnitude less than the amount that deposited in the N_2O_4 tests. Thus the tendency for flow decay to occur seems closely related to the amount of tracer that deposits.

Since some of the N_2O_4 tests suggested that considerable propellant may flow normally through the filter before flow decay begins, every effort was made to give flow decay a chance to occur. All of the runs of Table 9 were made using the same two gallons of N_2H_4 and the same filter employed in the initial run (run 22). The propellant was simply recirculated through the filter with a new run number assigned whenever additional radioactive tracer was added to the N_2H_4. The heat exchanger was set at as low a temperature as was practical (43°F) in runs 25(c)-(g). (N_2H_4 freezes at about 36°F). After many passes through the filter the flow rate was doubled in run 25(g) to see if the increased flow rate might induce flow decay as was observed in run 9(h) of the N_2O_4 tests. The results, however, were negative.

Metal salts are reported to be much more soluble in N_2H_4 than in N_2O_4.[4] It seems quite possible that flow decay does not occur in N_2H_4 because the metal contaminants never reach a state sufficiently close to saturation. To verify this idea attempts were made to prepare a solution of $ZnSO_4$ close to the saturation limit and then pass this solution through a filter (run 27). Zinc sulfate was selected as the salt because this substance is soluble to the extent of only about 70 ppm (as Zn) in N_2H_4 at room temperature.[4] The solution was prepared by dissolving 1g of $ZnSO_4 \cdot 7H_2O$ in 1 ml of H_2O and adding this solution to two gallons of N_2H_4. This would produce a solution of 28 ppm (as Zn). After adding the aqueous $ZnSO_4$ solution to the N_2H_4 in the catch tank, the mixture was agitated for about 5 minutes. The solution was then passed through one of the 10 micron filters into the feed tank (bypassing the filter in the test section) to remove any particulate $ZnSO_4$ that might be present. When the propellant was next flowed from the feed tank through the test section considerable flow decay occurred (24%). Of interest was the fact that the radioactivity count level on the filter decreased substantially during the run (about 60%). The filter in the test section was the same filter used in runs 22-26, and appreciable radioactivity had deposited prior to run 27. The decrease in count rate is easily explained by intermolecular exchange between the zinc atoms of the $ZnSO_4$ solution and Zn^{65} atoms of the zinc compound adhering to the filter.

At the conclusion of run 27 the filter was removed and placed in a polyethylene bag for storage. No special precautions were taken to avoid exposure to the air. The external surface had a dark appearance, probably due to the deposition of some sort of a zinc sulfate-hydrazine complex. About 5 minutes later the dark coloration had disappeared, and the plastic bag had melted. Apparently the zinc complex had undergone air oxidation releasing sufficient heat to cause the melting.

The foil dissolution test (Table 10) was a failure due to the N_2H_4 becoming contaminated with extraneous particulate matter. When the N_2H_4 was passed through the filter, plugging occurred. An examination of the N_2H_4 revealed the presence of numerous small black particles in the propellant. These black particles were traced to two likely sources. Many of the black particles were rather dense and were ferromagnetic. These were introduced from the acid immersion bath used in the cleaning procedure. The particles had deposited on the flange where the flange overlaps the walls of the tank such that the particles could not be seen when the inside of the tank was first inspected. The remainder of the black particles were believed to have come from one or more valve O-rings that deteriorated. Figure 15 shows one such O-ring discovered just after the completion of run 28. The bits and pieces of the O-ring are distributed over the upper threads in the picture. The O-ring was Parker compound (Cat. No. B591-8). The fact that the O-ring was old and had been used in both the N_2O_4 and N_2H_4 tests of this program probably contributed to its deterioration.

4.2.3.6 Temperatures

In all of the flow tests the propellant in the feed tank was maintained at a temperature of 70 ±5°F. In the case of 0.2 gpm N_2O_4/filter tests in which a 32°F heat exchanger was used, the propellant had warmed to 49°F by the time the test section was reached. In the case of 0.2 gpm N_2H_4/filter tests in which a 43°F heat exchanger was used, the propellant had warmed to 52°F prior to entry into the test section. The ΔT's across the filters and capillaries were small, corresponding to no more than a 1°F temperature rise.

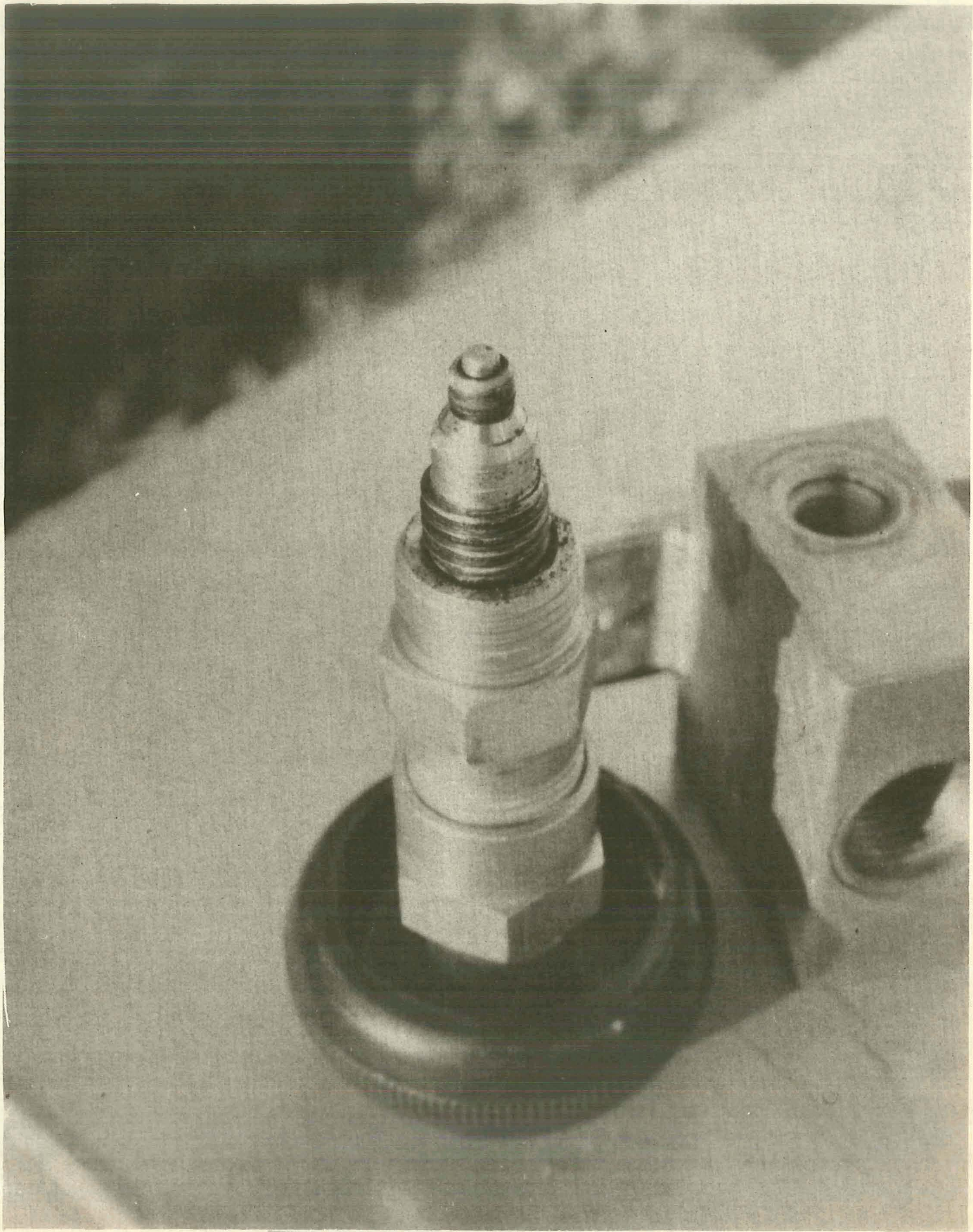

Figure 15: VALVE AND DETERIORATED O-RING

5.0 CONCLUSIONS

The thermal neutron activation analytical technique developed in Task 1 is an excellent method for the quantitative analysis of trace concentrations of metals in propellants. Although capable of high sensitivity, the method must be properly applied to reap fully this advantage. Due care must be exercised in choosing a container material, since impurities in the container may activate to give interfering gamma emissions. There is no reason, however, why the activated contents (e.g., propellant or aqueous solution of a standard) cannot be transferred to an inert (radioactively speaking) container for counting.

The "wet" analytical method, in which the liquid propellant and its contents are activated, should be avoided if possible. Besides the added handling difficulties, the method suffers from disadvantages such as instability of the propellant in the presence of reactor radiation (as was found for N_2H_4 in this program) and interference from the gamma emissions of volatile impurities (as was found for N_2O_4 in this program). However, the "dry" analytical method, in which the residue left after evaporating the propellant is activated, is quite satisfactory. The method minimizes propellant handling without any appreciable impact on either sensitivity or accuracy.

Atomic absorption spectroscopy, the only possible competitor of activation analysis in terms of sensitivity, yields results more rapidly. However, when lower detection limits are required or when a propellant sample must be analyzed for several metals simultaneously, then dry activation analysis is the correct choice. If a propellant sample must be analyzed in a nondestructive fashion, then wet activation analysis is a possible method in spite of its disadvantages.

The results of Task 2 show that radioactive tracers can be considered to have two major advantages as a diagnostic tool when applied to flow decay problems: (1) the high penetrability of gamma rays permits the movement of metal contaminants within a feed system to be externally monitored without disturbing the system in any way; and (2) the very high sensitivity of the tool permits a study of the movement of amounts of contaminants so small as to be orders of magnitude below the detection limits measured by other means.

The experimental results lead one to conclude that the MSC-PPD-2A N_2O_4 used in this program is highly prone to undergo flow decay when passed through 10 micron absolute filters. Distillation of the propellant is a means of eliminating the occurrence of flow decay, provided that the post-distillation contact time between the N_2O_4 and metal surfaces is short enough to avoid recontaminating the propellant with critical amounts of dissolved metals such as iron. The ease with which nitrates of radioactive zinc and chromium deposited on the filters indicates that these metals as well as iron can be found in N_2O_4 flow decay deposits. Since analytical data taken from this program and another[2] indicates that the concentrations of zinc and chromium (especially chromium) in N_2O_4 tend to be lower than that of iron, one would expect that these two metals play a smaller role in inducing flow decay.

Monitoring the movement of these radioactive contaminants allowed two important conclusions to be reached which help shed light on the flow decay mechanism. First, the amount of contaminant that need deposit to cause flow decay is only a small fraction (about 1 to 10%) of the metal content in solution. Second, of the 1 to 10% of the metal contaminant that deposits, the bulk of this material often deposits prior to the point at which a decrease in flow rate can be measured. More information is needed, however, before an actual mechanism can be postulated.

Flow decay appears not to be a problem when MIL-P-26536C N_2H_4 is passed through 10 micron filters. This conclusion is based on the fact that no flow decay was observed with N_2H_4 under the test conditions in this program and because far less radioactive material deposited in the N_2H_4 tests as compared to the N_2O_4 tests.

Although flow rate irregularities were experienced on occasion when both N_2O_4 and N_2H_4 were passed through 0.008 inch I.D. capillaries, these irregularities were more consistent with partial blockage by extraneous particulate matter in the propellant rather than the result of some flow decay mechanism. Placing a 10 micron filter upstream of the capillary would eliminate the flow irregularities in the case of N_2H_4, but would only compound the problem in the case of N_2O_4, since the filter would undergo blockage.

6.0 RECOMMENDATIONS

No further study of activation analysis as a means of quantitatively analyzing for metals in propellants is recommended. The various advantages and problem areas were adequately defined during Task 1 of this program.

Much remains unknown concerning flow decay mechanisms. The radioactive tracer technique was shown in this program to be an excellent tool for gaining insight into these mechanisms, and use of this tool should be pursued to gain additional insight. Flow tests conducted in Task 2 were limited to a narrow range of temperature and flow rate, and it would therefore seem desirable to broaden the data to include these important parameters. Other propellants should also be studied. Flow decay has not been observed in certain propellants, but the use of a more sensitive technique may uncover some hitherto unrecognized problems. Finally, other metals should be investigated. Aluminum and titanium alloys are important candidates because of their widespread use in the aerospace industry.

7.0 REFERENCES

1. "Methods for Elimination of Corrosion Products of Nitrogen Tetroxide," Rocketdyne Technical Report AFRPL-TR-67-277, July 1967.
2. "Investigation of the Formation and Behavior of Clogging Material in Earth and Space Storable Propellants," TRW Report 08113-6007-R000, October 1967.
3. "Study of the Dissolution Rate of Iron in N_2O_4 by the Use of Radioactive Tracers," Boeing Report D2-114478-1, January 1969.
4. "Investigation of the Formation and Behavior of Clogging Material in Earth and Space Storable Propellants," TRW Report 08113-6016-R000, October 1968.
5. "Analysis of Radiation Effects on Stored Liquid Propellants on Spacecraft With Auxiliary RTG or Nuclear Power Sources," Battelle Memorial Institute, NASA Contract NAS7-577, final report, May 31, 1968.
6. "Radiation Effects on Liquid Propellants," Battelle Memorial Institute, NASA Contract NAS7-722, final report, February 2, 1970.
7. W. S. Lyon, Jr., ed., Guide to Activation Analysis, D. Van Nostrand Co., Inc., Princeton, New Jersey, 1964.
8. "Flow Decay: Impaired Flow in Nitrogen Tetroxide Propulsion Systems Caused by Corrosion Product Deposits," Rocketdyne Technical Report AFRPL-TR-68-220, November, 1968.
9. "Nitrogen Tetroxide Corrosion Products," Rocketdyne Technical Report AFRPL-TR-69-114, February, 1969.
10. "Nitrogen Tetroxide Flow Decay Study for the Orbital Workshop Propulsion System," TRW Report 12243-6002-R000, June, 1969.
11. "Investigation of the Formation and Behavior of Clogging Material in Earth and Space Storable Propellants," TRW Report 08113-6025-R000, November, 1969.

DISTRIBUTION LIST FOR FINAL REPORT

CONTRACT NAS7-779

COPIES	RECIPIENT	DESIGNEE
	NASA HEADQUARTERS WASHINGTON, D.C. 20546	
1	CONTRACTING OFFICER	(X)
	NASA LEWIS RESEARCH CENTER 21000 BROOKPARK RD. CLEVELAND, OHIO 44135	
1	OFFICE OF TECHNICAL INFORMATION	(X)
	NASA MANNED SPACECRAFT CENTER HOUSTON, TEXAS 77058	
1	OFFICE OF TECHNICAL INFORMATION	(X)
	NASA MARSHALL SPACE FLIGHT CENTER HUNTSVILLE, ALABAMA 35812	
2	OFFICE OF TECHNICAL INFORMATION, MS-IP	(X)
1	TECHNICAL LIBRARY	(X)
1	DALE BURROWS S+E-ASTN-PJ	(X)
	NASA AMES RESEARCH CENTER MOFFET FIELD, CALIF. 94035	
1	PATENTS AND CONTRACTS MANAGEMENT	(X)
	JET PROPULSION LABORATORY 4800 OAK GROVE DR. PASADENA , CALIF. 91103	
4	LOUIS TOTH	(X)
3	MANAGER, LIQUID ROCKET PROPULSION TECH., CODE RPL OFFICE OF ADVANCED RESEARCH AND TECHNOLOGY NASA HEADQUARTERS WASHINGTON, D.C., 20546	(X)
1	DIRECTOR, TECHNOLOGY UTILIZATION DIVISION OFFICE OF TECHNOLOGY UTILIZATION NASA HEADQUARTERS WASHINGTON, D.C. 20546	(X)

25	NASA SCIENTIFIC AND TECHNICAL INFORMATION FACILITY P.O. BOX 33 COLLEGE PARK, MARYLAND 20740	(X)
1	DIRECTOR , LAUNCH VEHICLES AND PROPULSION , SV OFFICE OF SPACE SCIENCE AND APPLICATIONS NASA HEADQUARTERS WASHINGTON , D. C. 20546	(X)
1	DIRECTOR, ADVANCED MANNED MISSIONS, MT OFFICE OF MANNED SPACE FLIGHT NASA HEADQUARTERS WASHINGTON , D. C. 20546	(X)
1	MISSION ANALYSIS DIVISION NASA AMES RESEARCH CENTER MOFFETT FIELD, CALIFORNIA 24035	(X)

NASA FIELD CENTERS

1	AMES RESEARCH CENTER MOFFETT FIELD, CALIFORNIA 94035	HANS M. MARK
1	GODDARD SPACE FLIGHT CENTER GREENBELT, MARYLAND 20771	MERLAND L. MOSESON CODE 620
2	JET PROPULSION LABORATORY CALIFORNIA INSTITUTE OF TECHNOLOGY 4800 OAK GROVE DRIVE PASADENA, CALIFORNIA 91103	HENRY BURLAGE, JR PROPULSION DIV. 38
2	JOHN F. KENNEDY SPACE CENTER, NASA COCOA BEACH, FLORIDA 32931	DR. KURT H. DEBUS
2	LANGLEY RESEARCH CENTER LANGLEY STATION HAMPTON, VIRGINIA 23365	ED CORTWRIGHT DIRECTOR
2	LEWIS RESEARCH CENTER 21000 BROOKPARK ROAD CLEVELAND, OHIO 44135	LIBRARY
2	MARSHALL SPACE FLIGHT CENTER HUNTSVILLE, ALABAMA 35812	HANS G. PAUL CODE R-P+VED
2	MANNED SPACECRAFT CENTER HOUSTON, TEXAS 77058	J.G. THIBODAUX, JR. CHIEF, PROP. + POWER DIV. H. POHL

GOVERNMENT INSTALLATIONS

1	HEADQUARTERS, U.S. AIR FORCE WASHINGTON 25, D.C. 20546	COL.C.K. STAMBAUGH AFRST
1	ARNOLD ENGINEERING DEVELOPMENT CENTER ARNOLD AIR FORCE STATION TULLAHOMA, TENNESSEE 37388	DR. H.K. DOETSCH
2	AIR FORCE ROCKET PROPULSION LABORATORY RESEARCH AND TECHNOLOGY DIVISION AIR FORCE SYSTEMS COMMAND EDWARDS, CALIFORNIA 93523	RPRPD/MR. H. MAIN
1	AIR FORCE MISSILE TEST CENTER PATRICK AIR FORCE BASE, FLORIDA	L.J. ULLIAN
1	AERONAUTICAL SYSTEMS DIVISION AIR FORCE SYSTEMS COMMAND WRIGHT-PATTERSON AIR FORCE BASE DAYTON, OHIO 45433	D.L. SCHMIDT CODE ASRCNC-2
1	SPACE AND MISSILE SYSTEMS ORGANIZATION AIR FORCE UNIT POST OFFICE LOS ANGELES 45, CALIFORNIA 90045	COL. CLARK TECHNICAL DATA CENTER
1	DEFENSE DOCUMENTATION CENTER HEADQUARTERS CAMERON STATION, BUILDING 5 5010 DUKE STREET ALEXANDRIA, VIRGINIA 22314 ATTN- TISIA	
1	BUREAU OF NAVAL WEAPONS DEPARTMENT OF THE NAVY WASHINGTON , D. C. 20546	J. KAY RTMS-41
1	U.S. NAVAL ORDNANCE TEST STATION CHINA LAKE CALIFORNIA 93557	CODE 4562 CHIEF, MISSILE PROPULSION DIV.
1	PICATINNY ARSENAL DOVER, NEW JERSEY 07801	I. FORSTEN, CHIEF LIQUID PROPULSION LABORATORY,
1	U.S. ARMY MISSILE COMMAND REDSTONE ARSENAL ALABAMA 35809	MR. WALTER WHARTON

CPIA

1	CHEMICAL PROPULSION INFORMATION AGENCY APPLIED PHYSICS LABORATORY 8621 GEORGIA AVENUE SILVER SPRING, MARYLAND 20910	TOM REEDY

INDUSTRY CONTRACTORS

1	AEROJET-GENERAL CORPORATION P. O. BOX 296 AZUSA, CALIFORNIA 91703	W. L. ROGERS
1	AEROJET-GENERAL CORPORATION P. O. BOX 1947 TECHNICAL LIBRARY, BLDG 2015, DEPT. 2410 SACRAMENTO, CALIFORNIA 95809	R. STIFF
1	AEROJET-GENERAL CORPORATION SPACE DIVISION 9200 EAST FLAIR DR. EL MONTE, CALIFORNIA 91734	S. MACHLAWSKI
1	AEROSPACE CORPORATION 2400 EAST EL SEGUNDO BOULEVARD P. O. BOX 95085 LOS ANGELES, CALIF. 90045	JOHN G. WILDER MS-2293 D. JAEGER BLDG. A-2
1	AVCO SYSTEMS DIVISION WILMINGTON, MASSACHUSETTS	HOWARD B. WINKLER
1	BATTELLE MEMORIAL INSTITUTE COLUMBUS LABORATORIES 505 KING AVENUE COLUMBUS, OHIO 43201	LIBRARY
1	BEECH AIRCRAFT CORPORATION BOULDER DIVISION BOX 631 BOULDER , COLORADO	J. H. RODGERS
1	BELL AEROSYSTEMS COMPANY P.O. BOX 1 BUFFALO, NEW YORK 14240	W. M. SMITH
1	BELLCOMM 955 L-ENFANT PLAZA, S. W. WASHINGTON, D. C.	H. S. LONDON
1	BENDIX SYSTEMS DIVISION BENDIX CORPORATION 3300 PLYMOUTH ROAD ANN ARBOR, MICHIGAN 48105	JOHN M. BRUEGER
2	BOEING COMPANY P. O. BOX 3999 SEATTLE, WASHINGTON 98124	J. D. ALEXANDER LIBRARY
1	MISSILE DIVISION CHRYSLER CORPORATION P. O. BOX 2628 DETROIT, MICHIGAN 48231	MR. JOHN GATES
1	WRIGHT AERONAUTICAL DIVISION CURTISS-WRIGHT CORPORATION WOOD-RIDGE, NEW JERSEY 07075	G. KELLEY

1	RESEARCH CENTER FAIRCHILD HILLER CORPORATION GERMANTOWN, MARYLAND	RALPH HALL
1	REPUBLIC AVIATION CORPORATION FAIRCHILD HILLER CORPORATION FARMINGDALE, LONG ISLAND, NEW YORK	LIBRARY
1	GENERAL DYNAMICS, CONVAIR DIVISION P. O. BOX 1128 SAN DIEGO, CALIFORNIA	LIBRARY
1	MISSILE AND SPACE SYSTEMS CENTER GENERAL ELECTRIC COMPANY VALLEY FORGE SPACE TECHNOLOGY CENTER P.O. BOX 8555 PHILADELPHIA, PA.	F. MEZGER F. E. SCHULTZ
1	GRUMMAN AIRCRAFT ENGINEERING CORP. BETHPAGE, LONG ISLAND NEW YORK 11714	JOSEPH GAVIN
1	HONEYWELL, INC. AEROSPACE DIV. 2600 RIDGWAY RD MINNEAPOLIS, MINN.	MR. GORDON HARRIS
1	HUGHES AIRCRAFT CO. AEROSPACE GROUP CENTINELA AND TEALE STREETS CULVER CITY, CALIF. 90230	E. H. MEIER V.P. AND DIV. MGR., RESEARCH + DEV. DIV.
1	IIT RESEARCH INSTITUTE 10 WEST 35TH STREET CHICAGO, ILLINOIS 60616	LIBRARY
1	WALTER KIDDE AND COMPANY, INC. AEROSPACE OPERATIONS 567 MAIN STREET BELLEVILLE, NEW JERSEY	R. J. HANVILLE DIR. OF RESEARCH ENGR.
1	LING-TEMCO-VOUGHT CORPORATION P. O. BOX 5907 DALLAS, TEXAS, 75222	LIBRARY
1	MIDWEST RESEARCH INSTITUTE 425 VOLKER BLVD. KANSAS CITY, MISSOURI 64116	LIBRARY
1	ARTHUR D. LITTLE, INC. 20 ACORN PARK CAMBRIDGE, MASSACHUSETTS 02140	LIBRARY
1	LOCKHEED MISSILES AND SPACE CO. ATTN-TECHNICAL INFORMATION CENTER P.O. BOX 504 SUNNYVALE, CALIFORNIA 94088	J. GUILL S. DE BROCK
1	LOCKHEED PROPULSION COMPANY	LIBRARY

	P. O. BOX 111 REDLANDS, CALIFORNIA 92374	
1	THE MARQUARDT CORPORATION 16555 SATICOY STREET VAN NUYS ,CALIF. 91409	LIBRARY
1	BALTIMORE DIVISION MARTIN MARIETTA CORPORATION BALTIMORE, MARYLAND 21203	MR. JOHN CALATHES (3214)
1	DENVER DIVISION MARTIN MARIETTA CORPORATION P. O. BOX 179 DENVER, COLORADO 80201	DR MORGANTHALER A. J. KULLAS
1	ORLANDO DIVISION MARTIN MARIETTA CORP. BOX 5837 ORLANDO, FLORIDA	J. FERM
1	ASTROPOWER LABORATORY MCDONNELL-DOUGLAS CORP. 2121 PAULARINO NEWPORT BEACH, CALIFORNIA 92663	DR. GEORGE MOC
1	MCDONNELL-DOUGLAS CORP. P. O. BOX 516 MUNICIPAL AIRPORT ST. LOUIS, MISSOURI 63166	R. A. HERZMARK
1	SPACE+INFORMATION SYSTEMS DIVISION NORTH AMERICAN ROCKWELL 12214 LAKEWOOD BOULEVARD DOWNEY, CALIFORNIA 90241	LIBRARY
1	ROCKETDYNE (LIBRARY 586-306) 6633 CANOGA AVENUE CANOGA PARK, CALIF. 91304	DR. R. J. THOMPSON S. F. IACOBELLIS
1	NORTHROP SPACE LABORATORIES 3401 WEST BROADWAY HAWTHORNE, CALIFORNIA 90250	DR. WILLIAM HOWARD
1	AERONEUTRONIC CORPORATION PHILCO CORPORATION FORD ROAD NEWPORT BEACH, CALIFORNIA 92663	LIBRARY
1	ASTRO-ELECTRONICS DIVISION RADIO CORPORATION OF AMERICA PRINCETON, NEW JERSEY 08540	Y. BRILL
1	ROCKET RESEARCH YORK CENTER REDMOND, WASHINGTON 98052	F. MCCULLOUGH, JR.
1	SCIENTIFIC SERVICE BUREAU INC P. O. BOX 375 MORRISPLAINS, NEW JERSEY 07950	T. F. SEAMANS

1	SOUTHWEST RESEARCH INSTITUTE POST OFFICE DRAWER 28510 SAN ANTONIO, TEXAS 78228	LIBRARY
1	STANFORD RESEARCH INSTITUTE 333 RAVENSWOOD AVENUE MENLO PARK, CALIFORNIA 94025	DR. GERALD MARKSMAN
2	TRW SYSTEMS GROUP TRW INCORPORATED ONE SPACE PARK REDONDO BEACH, CALIF. 90278	G. W. ELVERUM LIBRARY
1	TAPCO DIVISION TRW, INCORPORATED 23555 EUCLID AVENUE CLEVELAND, OHIO 44117	P. T. ANGELL
1	THIOKOL CHEMICAL CORP AEROSPACE SERVICES ELKTON DIVISION BRISTOL, PENNSYLVANIA	LIBRARY
1	THIOKOL CHEMICAL CORPORATION HUNTSVILLE DIVISION HUNTSVILLE, ALABAMA 35807	JOHN GOODLOE
1	RESEARCH LABORATORIES UNITED AIRCRAFT CORP. 400 MAIN ST. EAST HARTFORD, CONN. 06108	LIBRARY
1	HAMILTON STANDARD DIVISON UNITED AIRCRAFT CORP. WINDSOR LOCKS, CONN. 06096	MR. R. HATCH
1	UNITED TECHNOLOGY CENTER 587 METHILDA AVENUE P. O. BOX 358 SUNNYVALE, CALIFORNIA 94088	DR. DAVID ALTMAN
1	FLORIDA RESEARCH AND DEVELOPMENT PRATT AND WHITNEY AIRCRAFT UNITED AIRCRAFT CORPORATION P. O. BOX 2691 WEST PALM BEACH, FLORIDA 33402	R.J. COAR
1	VICKERS, INC. BOX 302 TROY, MICHIGAN	LIBRARY